Technologies and Processes for the Advancement of Materials

Thermal processing

ISSUE FOCUS ///

GEAR APPLICATIONS / INSPECTION & METROLOGY

AFFORDABLE POWER DENSIFICATION IN STEEL COMPONENTS

COMPANY PROFILE ///

CeraMaterials

DECEMBER 2019
thermalprocessing.com

The Global Market Leader in Mission-Critical Integrated Heat Treatment Solutions

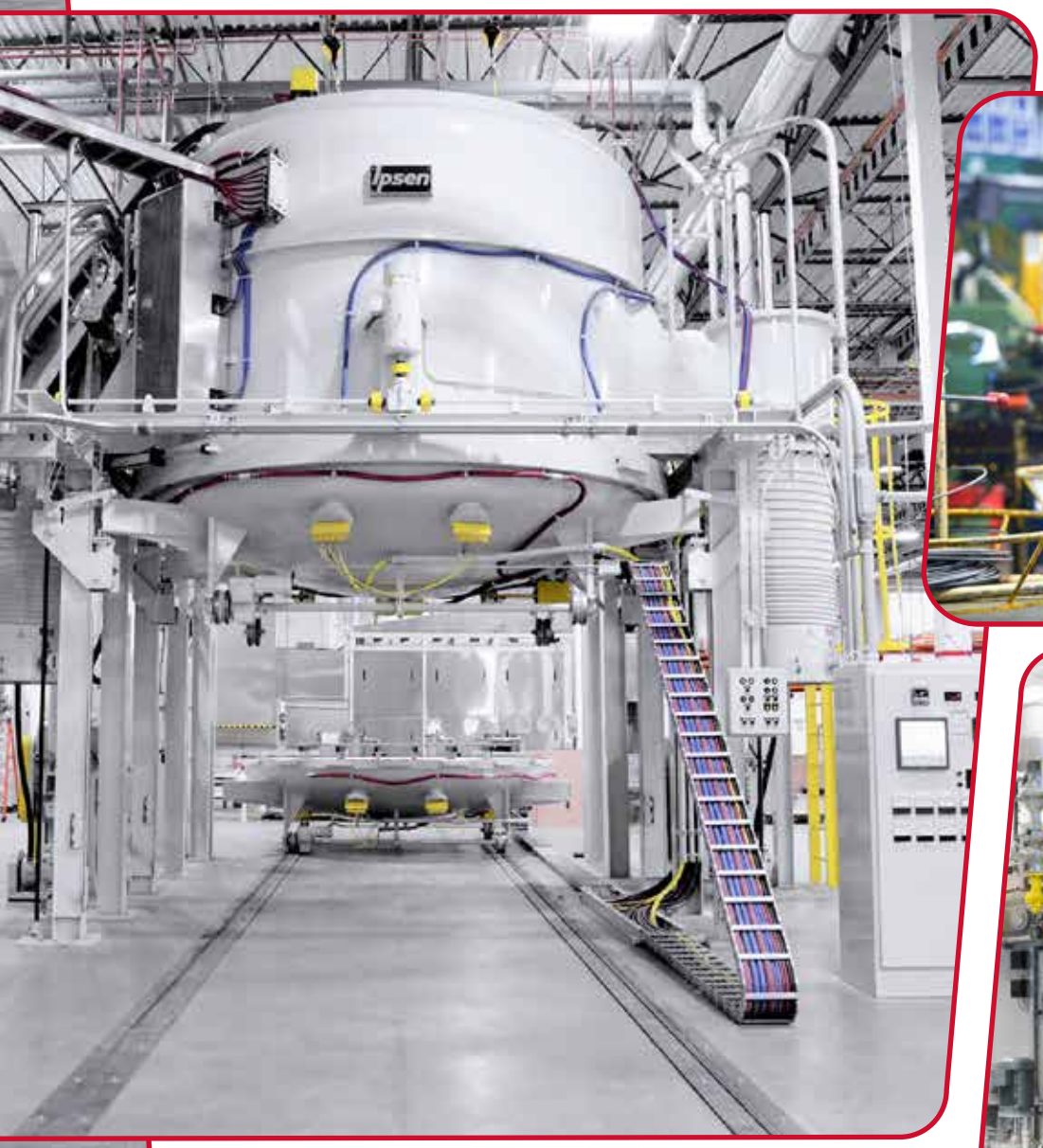

Backed by 70 years of experience, it is our mission to strengthen materials through expert-driven solutions. We are committed to delivering proven technology for a range of applications that enable you to transform space exploration, improve titanium medical implants and develop more efficient cars and jet engines.

Vacuum Atmosphere Customer Service Parts Rebuilds & Retrofits Controls

Ipsen

Sales@IpsenUSA.com | 815-332-4941 | IpsenUSA.com

Surface®
Furnace Solutions For Aluminum

Automotive/CQI-9

Aerospace/Nadcap

High Pressure Die Casting (HPDC)

Fixtureless T5/T6 Lines

Automated Quick Quench Batch Lines

Drop Bottom Furnaces

H-13 Die Casting & Extrusion Dies
- Nitriding (Gas or Ion) Surface Treatment
- Vacuum Heat Treatment

Surface® Combustion has earned a trusted reputation over 100 years of providing rugged, reliable thermal processing equipment and advanced technology backed by strong technical solutions. Surface applies this solutions orientation to a variety of physical materials needs including the manufacturing of processing equipment and systems for aluminum materials.

Surface's customers include the most well known aluminum companies in the world including highly respected automotive and aerospace component manufacturers. Whatever aluminum or non-ferrous heat processing technologies are needed, Surface has the equipment and engineering expertise to achieve the optimum solution yielding excellent product quality while maintaining the highest levels of production. Let us show you the **Value of Surface.**

Surface® Combustion

Engineered to Perform. Built to Last.

value@surfacecombustion.com
1-800-537-8980

surfacecombustion.com

CONTENTS ///

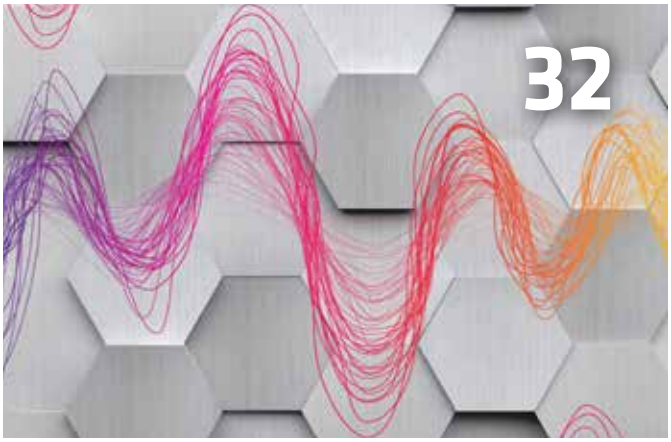

COVER PHOTO: SHUTTERSTOCK

DEPARTMENTS ///

DECEMBER 2019 VOLUME 8 / NUMBER 12

UPDATE ///

New Products, Trends, Services & Developments

Q&A ///

RAYMOND DANIEL NOBLE

VICE PRESIDENT ///
NOBLE INDUSTRIAL FURNACE

RESOURCES ///

Industrial Heating Equipment Association (IHEA)

In this section, the national trade association representing the major segments of the industrial heat processing equipment industry shares news of the organization's activities, upcoming educational events, and key developments in the industry. **16**

HOT SEAT ///

Tramp elements of Ni, Cr, Mo, and Cu increase hardenability, but also increase the potential distortion of a part during heat treatment. **18**

QUALITY COUNTS ///

Proper procedures, careful records, and a thorough reading of the Nadcap guidelines make testing metallic materials a smooth process. **22**

Thermal Processing is published monthly by Media Solutions, Inc., 266D Yeager Parkway Pelham, AL 35124. Phone (205) 380-1573 Fax (205) 380-1580 International subscription rates: $105.00 per year. Postage Paid at Pelham AL and at additional mailing offices. Printed in the USA. POSTMASTER: Send address changes to *Thermal Processing* magazine, P.O. Box 1210 Pelham AL 35124. Return undeliverable Canadian addresses to P.O. Box 503 RPO West Beaver Creek Richmond Hill, ON L4B4R6.

ARE YOU MAXIMIZING YOUR EXPOSURE?

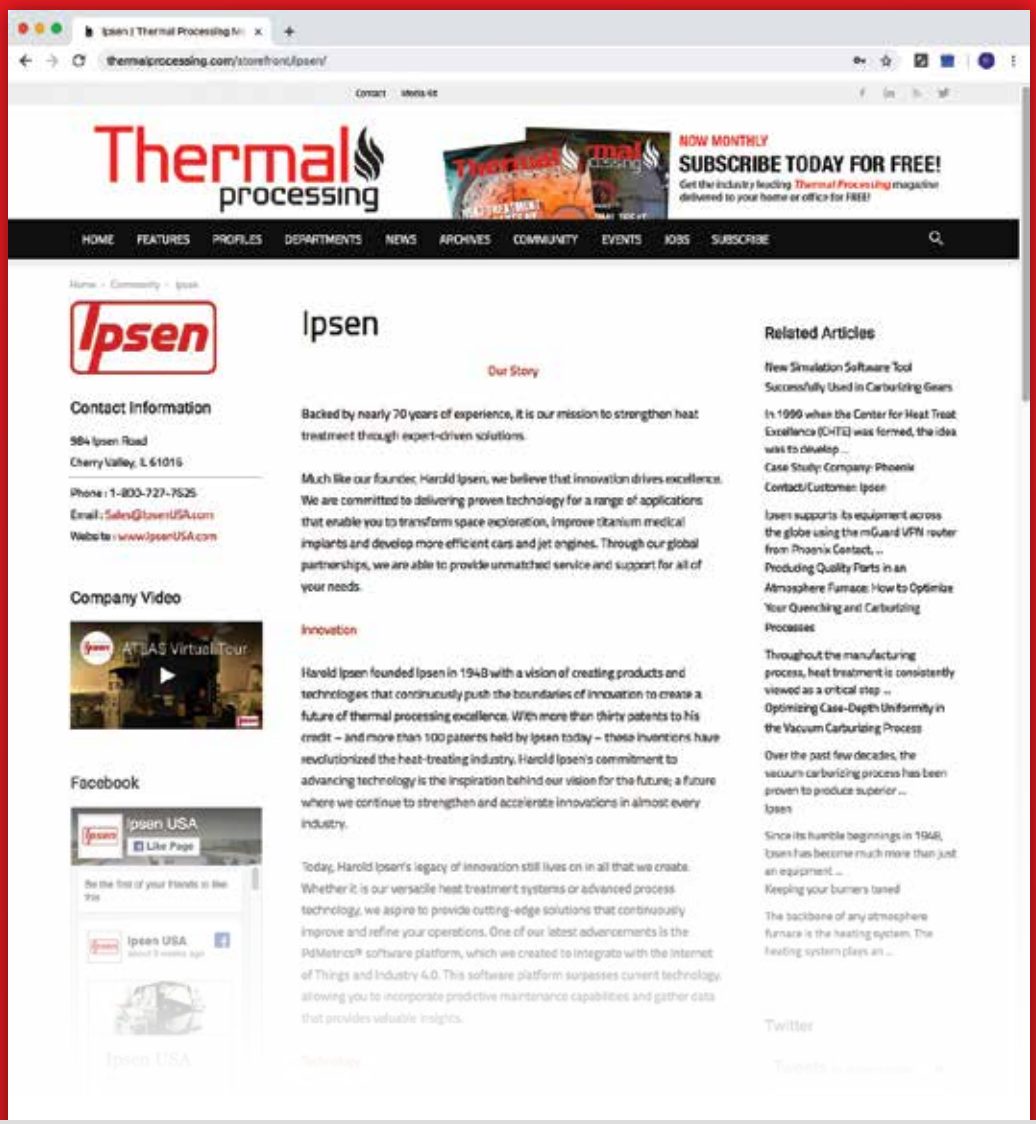

Connect your company to the heat treating industry with a storefront in the Thermal Processing Community.

Storefronts paint a portrait of your company with a 500-word description and include your logo, website link, phone number, email addresses, and videos. Your social media pages such as Twitter and Facebook are integrated with live updates, which may also be re-posted through our social media feeds.

With a community storefront, your company also receives a premium listing in the annual Buyer's Guide published each November. Premium listings feature graphic treatments to draw more attention to your company.

For information on how you can participate in the ThermalProcessing.com community storefront, contact

Dave Gomez – national sales manager
800.366.2185 ext. 207
dave@thermalprocessing.com

Thermal processing

FROM THE EDITOR ///

Happy holidays from Thermal Processing!

Looks like it's about time to put 2019 in the books, and looking back, it's been a busy year for us at *Thermal Processing* since we added six more issues to our annual publication schedule. Which means, for the first time, I can offer all our readers a proper salute to new beginnings as we enter 2020.

As we reflect on all the events of 2019, it's been a special year where we worked hard to bring you even more of the best heat-treat information you can use, whether it was in the form of detailed technical articles and columns or it was with the latest news within the heat-treat industry.

We really hope you've enjoyed the extra heat-treat coverage, and we plan to work even harder as we jump head first into the new year.

And as we close out our year here, you'll discover this month's issue of *Thermal Processing* has quite a bit to take in.

In this month's Focus section, we take a look at gear applications within the heat-treat industry. In that vein, Buddy Damm shares his insights on combining strength and toughness for affordable power densification in steel components.

In December's company profile, we talk to the president of CeraMaterials. This company has been specializing in high-temperature refractory materials for several years now and is becoming quite the player within the industry. I am proud to share their success story with you.

I'm also proud to present our newest columnist: D. Scott MacKenzie. He has agreed to pull double duty by writing *Thermal Processing's* Hot Seat column. If you are a reader of our sister publication, *Gear Solutions*, his name should sound familiar as he also writes *Gear's* Hot Seat column as well. I am excited to add his amazing expertise to our *Thermal Processing* family.

You'll find that and much more in our December issue. And keep in mind that we are always looking for interesting and educational editorial content, so if you have a technical paper or other heat-treat-related articles you'd like to see published, please contact me. I'd love to hear from you and be given the opportunity to share your unique knowledge with our readers.

Happy holidays from all of us at *Thermal Processing*, and, as always, thanks for reading!

KENNETH CARTER, EDITOR
editor@thermalprocessing.com
(800) 366-2185 x204

CALL FOR ARTICLES Have a technical paper or other work with an educational angle? Let Thermal Processing publish it. Contact the editor, Kenneth Carter, at *editor@thermalprocessing.com* for how you can share your expertise with our readers.

Thermal processing

David C. Cooper
PUBLISHER

Chad Morrison
ASSOCIATE PUBLISHER

EDITORIAL

Kenneth Carter
EDITOR

Jennifer Jacobson
ASSOCIATE EDITOR

Joe Crowe
CONTRIBUTING EDITOR

SALES

Chad Morrison
ASSOCIATE PUBLISHER

Dave Gomez
NATIONAL SALES MANAGER

CIRCULATION

Teresa Cooper
MANAGER

Jamie Willett
ASSISTANT

DESIGN

RIck Frennea
CREATIVE DIRECTOR

Michele Hall
GRAPHIC DESIGNER

CONTRIBUTING WRITERS

ZHICHAO CAI
HAO CHENG
E. BUDDY DAMM
CHENGCHENG LIU
D. SCOTT MACKENZIE
JASON SCHULZE

Media solutions

PUBLISHED BY MEDIA SOLUTIONS, INC.
P. O. BOX 1987 • PELHAM, AL 35124
(800) 366-2185 • (205) 380-1580 FAX

David C. Cooper
PRESIDENT

Chad Morrison
VICE PRESIDENT

Teresa Cooper
OPERATIONS

YOUR INDUSTRY NEWS SOURCE

Thermal Processing magazine is a trusted source for the heat treating industry, offering both technical and educational information for gear manufacturers since 2012.

Each issue, Thermal Processing offers its readers the latest, most valuable content available from companies, large and small, as well as critical thoughts on what this information means for the future of the heat treating industry.

Best of all, it's free to you. All you need to do is subscribe.

On ThermalProcessing.com, we have paired our vast technical archives with the latest web technologies to develop the most efficient, streamlined, user-friendly web experience in the gear industry.

SUBSCRIBE FOR FREE

www.thermalprocessing.com

Thermal processing

Allied Mineral Products' engineering capabilities include designing and manufacturing complex shapes in virtually any size. (Courtesy: Allied Mineral Products)

Allied Mineral Products opens precast shapes plant

Allied Mineral Products opened the doors to its newest precast shapes manufacturing facility near Johannesburg, South Africa. This marks Allied's sixth precast shapes location worldwide.

Shapes manufacturing brings an added benefit to South African customers. Some benefits include foundry crucibles, furnace structural parts, EAF deltas and spouts, tilters and skimmer blocks, dampers and divider walls, incinerator shapes, and rotary furnace shapes.

Allied's engineering capabilities include designing and manufacturing complex shapes in virtually any size. Precast shapes can also be created from existing drawings or shapes.

Allied Mineral Products is a leading global manufacturer of monolithic refractories and precast refractory shapes with 12 worldwide manufacturing facilities, six precast shapes facilities, and three research and technology centers. Headquartered in Columbus, Ohio, Allied serves a wide variety of industries with innovative refractory solutions and exceptional service and support, backed by expert engineering and research teams. Allied is an employee-owned company.

MORE INFO www.alliedmineral.com

Grieve offers 1,050°F two-drawer cabinet oven for annealing

Grieve No. 1049 is a 1,050°F (566°C) cabinet oven with two drawers, currently used for annealing or normalizing processes at the customer's facility. Workspace dimensions of this oven measure 39" W x 102" D x 51" H, with two drawers rated 250 lbs. loading with 36" wide x 78" deep x 15" high loading area. 800,000 BTU/hour installed in a modulating natural gas burner, while a 10,000 CFM, 7-1/2 HP recirculating blower provides horizontal airflow to the workload.

This Grieve oven features 10-inch thick insulated walls comprised of 2-inch 2,000°F ceramic blanket and 8 inches of 10 lb/cf density rockwool. Features include a top-mounted heat chamber, aluminized steel exterior and Type 304, 2B finish stainless steel interior. Additional features include a rear door for access to workspace and heat chamber, exhaust hood over drawers, and motorized dampers on intake and exhaust for accelerated cooling.

The oven includes all safety equipment required by IRI, FM, and National Fire Protection Association Standard 86 for gas-heated equipment, including 1,800 CFM stainless steel powered forced exhauster. It also meets AMS2750, Class 2 (±10F), Type C (survey thermocouple at hottest and coldest location).

Controls on the No. 1049 include a digital indicating temperature controller, two digital shutdown timers, one for burner and one for oven, and a circuit breaker disconnect switch.

MORE INFO www.grievecorp.com

The Grieve No. 1049 includes all safety equipment required by IRI, FM, and National Fire Protection Association Standard 86 for gas-heated equipment.

SEND US YOUR NEWS Companies wishing to submit materials for inclusion in Thermal Processing's Update section should contact the editor, Kenneth Carter, at editor@thermalprocessing.com. Releases accompanied by color images will be given first consideration.

Companies announce high-temp aluminum alloy for AM

In a joint effort, QuesTek Innovations LLC and the German Aerospace Center will explore the full potential of QuesTek's new printable aluminum (Al) alloy. QuesTek Innovations LLC, a leading developer of metal alloys, announced that it has developed the new aluminum alloy for additive manufacturing. This alloy is capable of high-strength performance at elevated temperatures (200-300°C) in the as-built condition. It is believed to be the first powdered AI material to meet those requirements without the need for subsequent heat treatment. The new alloy will enable the printing of lighter-weight precision components not currently possible with traditional manufacturing methods. Examples include heat exchangers or other components requiring internal cooling channels, where such features are not viable to obtain via machining. Because of the high-temperature strength of printed components using QuesTek's new alloy, it will also be possible to reduce weight in parts that currently must be made from titanium.

The new Al alloy was developed using QuesTek's proven Integrated Computational Materials Engineering (ICME) technologies and Materials by Design® approach, which combines the company's computational technology with an exclusive stage-gate design and development process. As a global leader in the practical application of ICME, QuesTek focuses on the rapid design and development of materials, from a conceptual need through product insertion.

In an effort to explore the full potential of QuesTek's printable Al alloy, the company will be collaborating with the prestigious German Aerospace Center (Deutsches Zentrum für Luft-und Raumfahrt, "DLR"). The DLR will print demonstration components of its design for aeronautics and space applications, and prepare a performance brief for European aerospace manufacturers.

Commenting on the development, Greg Olson, QuesTek chief science officer, said, "The accelerated design and development of a printable aluminum alloy capable of meeting so many current needs is especially exciting, as it will enable concurrent design of material composition and component geometry. Based on our internal test results, we see broad application of this material in manufacturing components for aerospace, satellite, automotive and high-performance racing. We are particularly pleased to be collaborating with the DLR. Their unrivaled reputation, expertise, and close relationship with industry needs will bring an important new scope to our efforts."

Aerospace oil filter printed with new QuesTek Innovations' high-temperature AI alloy. (Courtesy: QuesTek)

Heinz Voggenreiter, director of the Institute of Materials Research for the DLR, said, "For additive manufacturing to become a production technology with the capacity to produce components capable of performing in high temperature, high-stress applications, new extraordinary printable alloys will be needed. The German Aerospace Center, with its decades of experience in the development of materials and structures for space and aeronautics, is an ideal cooperation partner for QuesTek to explore intended applications."

This new high-temperature Al alloy is one of a series of Al alloys for additive manufacturing QuesTek is developing, under multiple U.S. Navy-funded Small Business Innovation Research awards. Other Al alloys under development by QuesTek include a high strength at-room-temperature variant, as well as high strength and highly corrosion-resistant variant. QuesTek is also collaborating closely on high-temperature Al additive manufacturing alloys for engine applications with Pankl Racing, an Austrian-based manufacturer known for advanced production technologies and high-performance components.

MORE INFO www.questek.com

Oregon Products commissions new Can-Eng system

Oregon Products awarded Can-Eng Furnaces a contract to design and commission a new heat-treatment system for Oregon's production facilities.

Oregon, a leading global manufacturer of saw chain and other replacement products for the forestry industry, plans to use the new continuous high-capacity mesh belt austemper heat-treat equipment as part of a long-standing commitment to continuous quality improvement.

"The primary business driver of this project is quality. We sought out leading international thermal processing equipment suppliers to support our premium quality forestry cutting products which demand a high quality austempering system," said Kaitlyn McNaughton, director of engineering and R&D Labs. "This new furnace is primarily targeted to raise the bar on quality for our harvester chain products, which perform under the highest loads and most extreme conditions."

Through collaboration, Can-Eng International, Ltd. was favored largely due to its ability to demonstrate consistent bainitic structure metallurgical properties and advanced equipment design expertise, which allowed for a compact system foot-

Oregon Products recently awarded Can-Eng Furnaces International, Ltd. a contract to design and commission a new continuous high capacity mesh belt austemper heat treatment system for Oregon's production facilities. (Courtesy: Can-Eng)

print. The austemper system integrates a computerized loading system, pre-wash system, atmosphere-controlled mesh belt austenitizing furnace, molten salt quench conveyor system, post quench residual salt removal and recycling system, mesh belt parts drying oven, unloading system and Can-Eng's PET™ system (which provides vital features such as individual lot/product traceability), detailed process data collection for continuous process improvements, and comprehensive Industry 4.0 equipment diagnostics capability.

The system is scheduled for commissioning early 2020.

MORE INFO www.can-eng.com

Gasbarre supplies car bottom furnace to U.S. manufacturer

Gasbarre Thermal Processing Systems recently manufactured and commissioned a high temperature car bottom furnace for a Southern U.S. manufacturer of excavating equipment. The furnace has a work zone of 84 inches wide by 144 inches long by 48 inches high with a 16,000-pound load capacity. The operating temperature is 1,000°F (538°C) to 2,282°F (1250°C), and will be used for stress relieving, normalizing, and other high-temperature processes. The furnace was purchased to replace an existing furnace, which gave the customer improved operating efficiency and higher temperature processing capabilities. The heating system features low emissions gas-fired burners with a custom-designed control scheme to meet the customer's strict NOx and CO requirements. The furnace meets AMS 2750 temperature uniformity requirements across a wide temperature operating range, and was custom designed to fit into the customer's existing space in their facility.

Gasbarre Thermal Processing Systems in Plymouth, Michigan, has been designing, manufacturing, and servicing a full line of industrial thermal processing equipment for more than 40 years. Gasbarre's product offering includes both batch and continuous heat-processing equipment and specializes in temper, tip up, mesh belt, nitriding, box, car bottom, pit, and vacuum furnaces as well as a full line of replacement parts and auxiliary equipment which consists of atmosphere generators, washers, quench tanks, and charge cars. Gasbarre continues to service and support J. L. Becker brand equipment and custom designs and manufactures thermal processing equipment to meet customer's specific needs.

MORE INFO www.gasbarre.com

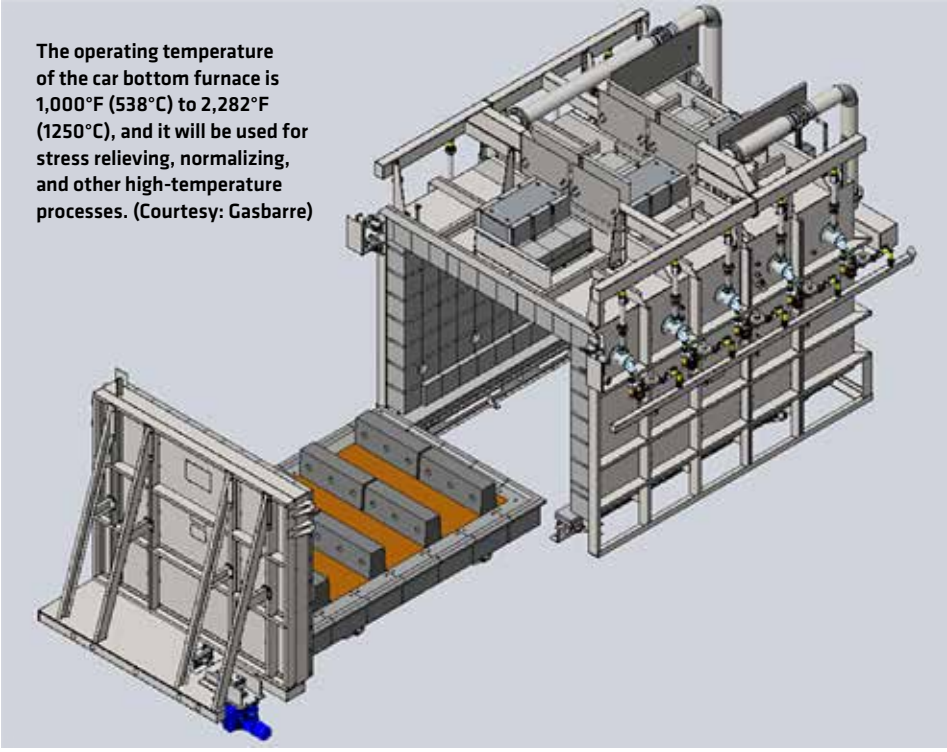

The operating temperature of the car bottom furnace is 1,000°F (538°C) to 2,282°F (1250°C), and it will be used for stress relieving, normalizing, and other high-temperature processes. (Courtesy: Gasbarre)

TPS ships Gruenberg depyrogenation sterilizers

Thermal Product Solutions, a global manufacturer of thermal-processing equipment, announced the shipment of two Gruenberg depyrogenation sterilizers to the pharmaceutical industry. The units will be used for sterilizing pharmaceutical equipment.

These pharmaceutical sterilizers have maximum temperature ratings of 280°C with work chamber dimensions of 36" W x 36" D x 53" H. The Gruenberg sterilizers were constructed from a structural steel frame that supported the 304L stainless steel interior chamber liner and the 304 #4 polished stainless-steel exterior. All interconnecting struts are non-continuous, which keeps the exterior cool.

Located in a plenum chamber in the top of the sterilizers, circulation blowers direct air through circulation ducts located on one side of the workspace. The air passes through high-temperature HEPA filters first, and then enters the chamber through a semi-pierced duct wall. The air flows horizontally across the product, exits through a

These Gruenberg pharmaceutical sterilizers have maximum temperature ratings of 280°C with work chamber dimensions of 36" W x 36" D x 53" H.

semi-pierced duct wall on the opposite side, and enters a recirculation duct. The air is then directed back to the blower for reheating and recirculation.

Rapid ramp HEPA filters on the circulation and exhaust air flow systems were added to allow the machines to ramp up to temperature and cool down at a rate of 5°C per minute. An Allen Bradley touchscreen HMI with PLC was installed on each unit for temperature and process control. The system was also supplied with an array of thermocouples to monitor the product inside of the chamber.

"These single door sterilizers were designed and tested to provide ISO 5 or Class 100 sterilizing conditions at ambient and operating temperatures," said Jonathan Young, Gruenberg product manager.

Features include:

› Stainless steel 304 with a #4 finish exterior.

› Fully welded 304L stainless steel interior liner.

› Removable floor stand.

› 4 inches of insulation.

› 3/4" radius corners.

› Pneumatic door locks.

› Air intake HEPA filter.

› Air exhaust HEPA filter.

› Circulation HEPA filter.

› Accelerated ramp feature.

› +/-5°C at 232°C temperature uniformity.

› NEMA 12 control console.

› Allen Bradley PLC and HMI.

› High limit thermostat.

› Fused main power disconnect switch.

› Yokogawa strip chart recorder.

› Monitoring thermocouples inside chamber.

› Tested for ISO 5 conditions.

MORE INFO www.thermalproductsolutions.com

L&L ships box furnace with inert atmosphere

L&L Special Furnace Co, Inc., has shipped a Model FB1046 floor-standing box furnace to a worldwide leader of high-tech aerospace and associated components located in the Southeastern United States. The furnace will be used for processing aerospace parts and various thermal applications.

The work zone is 120" wide by 48" high by 72" deep. The furnace has a temperature gradient of ±20 F from 1,100°F to 2,150°F using eight zones of temperature control with biasing to balance any differential in temperature gradients.

The furnace controller is a Eurotherm Nanodac program control/recorder that has 100 individual programs with up to 25 segments for each program. The furnace also has overtemperature protection with manual reset and backup safety contactors. There is a NEMA12 panel and fused disconnect.

The L&L Special Furnace Co.'s Model FB1046 will be used for processing aerospace parts and various thermal applications. (Courtesy: L&L Furnace)

The furnace has special slots that are cut into the door as a passthrough for atmosphere inlet and outlet tubes. This allows for inert atmosphere to flow directly into the customer's sealed parts manifold, and ensures good atmosphere circulation to the parts as they are being processed. The manifolds are supported on a series of castable piers located inside the furnace.

The furnace is rated for use to 2,200°F and includes a 1,200 CFM venturi for accelerated cooling. There is an electric counterbalanced vertical door with a floor switch for activation.

All of L&L's furnaces can be configured with options and specifically tailored to meet a customer's thermal needs. Furnaces may also be equipped with pyrometry packages to meet ASM2750E and soon-to-be-certified MedAccred guidelines.

Options include a variety of control and recorder configurations. A three-day, all-inclusive startup service is offered with each system within the continental U.S. and Canada. International startup and training service is available by factory quote.

MORE INFO www.llfurnace.com

Metal Exchange Corporation names Rick Merluzzi CEO

Metal Exchange Corporation (MEC) has promoted Rick Merluzzi to chief executive officer of MEC. Mike Lefton, current MEC chairman and CEO, will assume the title of executive chairman. Merluzzi oversees all Metal Exchange Corporation businesses, including Metal Exchange Trading, Pennex Aluminum Company, Continental Aluminum, and Electro Cycle, Inc. Merluzzi joined Metal Exchange Corporation 15 years ago as president of MEC subsidiary Pennex Aluminum Company, and for the past five years has served as president and chief operating officer of MEC.

"Much of our success at MEC can be attributed to Rick Merluzzi's outstanding leadership," said Lefton. "Rick builds high performing teams internally, and creates valued

partnerships externally. He is laser-focused on our vision to become an injury-free company, and has a passion for helping all in the MEC family reach their fullest potential.

"Rick's actions exemplify the Metal Exchange dual bottom line philosophy, where the safety, well-being, and fulfillment of everyone within MEC are held equal to our financial success. I have extreme confidence in Rick's ability to continue to lead Metal Exchange Corporation to new heights, as we continue our quest to impact our world and create raving fans," Lefton said.

"Metal Exchange has an incredible track record of success over its 45-year history. I am humbled and honored to work for this family-owned, people-focused organization, which has a long-term commitment to our industry," said Merluzzi. "We have grown substantially by focusing on helping our customers achieve success. This impressive growth is a direct result of the hard work and commitment of the many talented people throughout our company who embrace our core values of safety, integrity, respect and drive."

Rick Merluzzi

Metal Exchange Corporation is a private, family-owned company with global headquarters in St. Louis, Missouri. It is one of the most diverse providers of non-ferrous metals. Founded in 1974, Metal Exchange Corporation and its family of companies are industry leaders in non-ferrous metals, from purchasing to manufacturing and processing. With offices in Zurich, Shanghai and Singapore, Metal Exchange Corporation has the international presence needed to link suppliers and customers around the globe.

MORE INFO www.metalexchangecorp.com

Wisconsin Oven ships multi-zone curing ovens

Wisconsin Oven shipped two electrically heated multi-zone curing ovens to the composites industry. These ovens will be used to cure carbon fiber threads.

Wisconsin Oven shipped two electrically heated multi-zone curing ovens to the composites industry. (Courtesy: Wisconsin Oven)

One of the curing ovens has six zones, is rated for 250°C (482°F), and has work chamber dimensions of 19'0" wide x 16'4" long x 2'0" high. The second oven has two zones and is rated for 260°C (500°F) with work chamber dimensions of 19'0" wide x 41'4" long x 2'0" high. Guaranteed temperature uniformity of ± 5°C @ their respective maximum temperature ratings was documented with a profile test for both ovens.

The curing ovens each feature a wire mesh rolling filter system in each zone. The filter system is plug mounted for ease of removal and maintenance and uses exterior crank handles at each zone that are used to advance the material as needed. Both units were also designed with Wisconsin Oven's energy efficient E-Pack™ upgrade which includes thicker wall panels.

"The heating systems are wired so if a heater fails, the oven will operate at near full heat input until downtime can be scheduled. At Wisconsin Oven we understand the importance of minimizing downtime for maintenance and this design is intended to keep the equipment operational until it can be serviced," said Tom Trueman, senior applications engineer.

Features of the curing ovens include:

› Top-down air flow for optimal distribution along the product.

› Personnel access doors for ease of cleaning, maintenance and service.

› Wire mesh rolling filter system in each zone.

› E-Pack™ upgrade to improve energy efficiency.

› OSHA compliant ladder and railings to provide access to roof mounted blowers.

MORE INFO www.wisoven.com

Sandvik announces agreement with Serck Services (Gulf)

Sandvik's team based in Dubai has announced a new working partnership with heat exchanger manufacturer Serck Services (Gulf) based in Sharjah, United Arab Emirates.

This cooperation and supply agreement has been initiated to offer customers operating and maintaining heat exchangers a service whereby Sandvik will advise the best types of material and grades considering the process conditions, and Serck will

provide manufacturing expertise for producing the heat exchanger unit. As part of the arrangement, joint customer visits to process plants and refineries are to be carried out to enable true cooperation and close working practices.

Duplex tube-to-tube sheet welding is key to fabrication and Sandvik will offer this support as part of this agreement.

James Doughty, regional sales director, and Barinder Ghai, regional technical marketing manager, are leading the project for Sandvik. "Companies often require assistance and advice for the selection of the best materials for the application in which the equipment is going to be used. This partnership with Serck means that we are able to be involved in the planning and specification process at the outset and therefore ensuring the best outcome for the customer," Doughty said.

"This type of consultation with heat exchanger customers is something we are keen to expand upon as part of our service and is a further testament to the knowledge and expertise of our team," said Ghai.

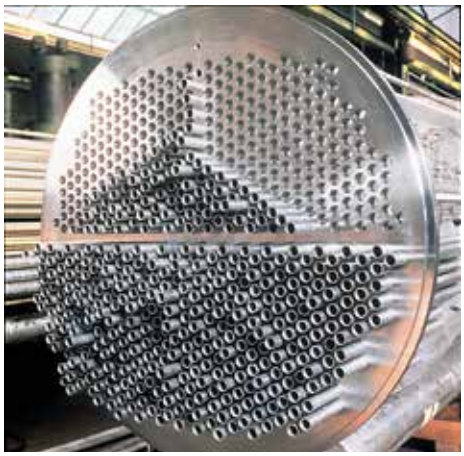

Sandvik announces cooperation and supply agreement with Serck Services (Gulf) for heat exchanger manufacture within the Middle East and North Africa (MENA) Region. (Courtesy: Sandvik)

"Getting the whole specification right at the outset is key to delivering an efficient and successful result for the customer and we believe that working closely with Sandvik on the material specification side is key to ensuring this," said Damian Murphy, business manager – Industrial Heating Manufacturing for Serck.

Rohith Chako, product manager at Sandvik, and Damian Murphy, business manager for Serck, will be the primary, day-to-day contacts for this initiative within the region.

Part of the Unipart Group and together with its sister branch networks in the UK and U.S., Serck is the only international heat transfer technology specialist in the Middle East and one of the largest automotive, industrial, and marine heat transfer companies in the world. Operations range from the production of automotive radiators through to the testing, servicing, re-tubing, and complete manufacture of industrial and marine heat exchangers.

MORE INFO www.materials.sandvik

Seco Super IQ®: No flames, no endogas, higher temps

Seco/Vacuum Technologies, Seco/Warwick Group's company, has introduced to the North American market Super IQ® (integral quench furnace), the industry's next-generation carburizing furnace with more built-in features. The American premiere took place in October at ASM2019 in Detroit.

The Super IQ offers all the benefits of low-pressure carburizing with none of the added costs. The system combines clean processing with the exceptional performance of oil quenching using the most innovative integral quench furnace design in decades. With a Super IQ, users get super-clean parts while still getting the benefit of a simple atmosphere oil quench without any additional costs.

"The concept for a new alternative to the integral quench furnace was born of calls from heat-treatment facility managers and owners demanding a cleaner, faster, more efficient method for carburizing. We introduced the Super IQ this year with a multitude of benefits over traditional methods, especially productivity: Because the Super IQ operates at higher temperature ranges, heat treaters can expect faster cycle times which translates into a more productive work center," said Jaros aw Talerzak, vice-president business segment thermal, Seco/Warwick.

Built-in benefits of Super IQ, the modern replacement for gas-fired integral quench, include:

› Carburizing with no flames and no endogas;

› Turn it on, turn it off – no idling or conditioning;

› Clean, cool, contained thermal cycling in vacuum;

› Nominal temperatures up to 2,000ºF;

› Integral quench using standard quench oils.

The Super IQ furnace is a hybrid system combining, in a single furnace, the best traits of a conventional IQ furnace with the clean processing of Seco/Warwick's Casemaster Evolution® multi-chamber vacuum furnace (flagship product on Seco/Warwick Group's portfolio). It is primarily designed for carburizing processes at elevated temperatures and hardening. The furnace features a traditional vestibule with automatic loading and oil quench, plus a vacuum-tight heating chamber and an oil quench. The furnace is designed so that it can be seamlessly integrated into an installed line of conventional furnaces using an existing loading system.

The Super IQ® will be offered to the American market from Seco/Vacuum Technologies LLC (SVT), a fully-owned entity of Seco/Warwick Group.

MORE INFO www.secovacusa.com

Built with Solar Manufacturing's SolarVac® Polaris control system and a graphite-insulated hot zone, the furnace is designed to accommodate loads up to 36" wide x 36" high x 48" deep, with a maximum weight of 5,000 pounds. (Courtesy: Solar Manufacturing)

Solar Manufacturing ships furnace to science/tech lab

Solar Manufacturing has shipped a vacuum furnace for processing additive manufactured parts to a large science and technology laboratory. The lab requires the furnace to further its research and development work. Built with Solar Manufacturing's SolarVac® Polaris control system and a graphite-insulated hot zone, the furnace is designed to accommodate loads up to 36" wide x 36" high x 48" deep, with a maximum weight of 5,000 pounds. Operating at a vacuum level of 10-5 torr, with maximum temperatures up to 2,400 °F, and quench pressure of two bar, the furnace will be commissioned by year's end.

"Solar Manufacturing was awarded the order because we offered the best solution for this customer's vacuum furnace needs," said Dan Insogna, Solar Manufacturing's Southeast sales manager. "Our knowledge and experience of the additive manufacturing market set us apart from the competition. We are pleased to provide a solution to the growing research and development efforts within the Additive Manufacturing Industry, and we know our Solar Manufacturing vacuum furnace is the right tool for job."

Solar Manufacturing designs and manufactures a wide variety of vacuum heat treating, sintering, and brazing furnaces and offers replacement hot zones, spare parts, and professional service.

MORE INFO www.solarmfg.com

Gasbarre takes partner to expand footprint in Mexico

Gasbarre Thermal Processing Systems has partnered with Humberto Bastidas from Thermal Technic Furnace Solutions. Customers can now experience the benefit of having a Mexico resident who speaks Spanish to provide the best possible customer service. Bastidas has many years of experience in the heat-treating field and marketplace. Gasbarre will be working with Bastidas and his team to launch a Spanish version of Gasbarre.com and will assist with other marketing efforts in that region.

Located in St. Marys, Pennsylvania, Gasbarre Thermal Processing Systems has

been designing, manufacturing, and servicing a full line of industrial thermal processing equipment for more than 40 years. Gasbarre's product offering includes both batch and continuous heat-processing equipment and specializes in temper, tip up, mesh belt, nitriding, box, car bottom, pit, and vacuum furnaces, as well as a full line of replacement parts and auxiliary equipment which consists of atmosphere generators, washers, quench tanks, and charge cars. Gasbarre continues to service and support Sinterite brand equipment and custom designs and manufactures thermal processing equipment to meet customers' specific needs.

MORE INFO www.gasbarre.com

Tenney vacuum drying oven reduces cycle

Tenney Environmental, a division of Thermal Product Solutions, has shipped a vacuum drying oven to the aerospace industry. This vacuum drying oven is designed to remove moisture from a large spacecraft engine after it goes through a washing process. The previous conventional method of drying took more than 12 hours due to the intricacy of small diameter tubing, fine screen meshes, and other hard-to-get-to areas. The vacuum drying oven will reduce that time to four hours.

This vacuum drying oven uses radiant heat wrapped around the pressure walls to heat the product to approximately 100°F. The chamber is also evacuated to a very low vacuum level and simultaneously purged with heated gaseous nitrogen via an on-board automated GN2 heater. Lowering the pressure around the product lowers the boiling point of the standing water in the hard-to-reach areas. This allows for the moisture to be boiled off much more quickly at a lower-than-normal boiling temperature so the product is not heated above safe operating temperatures. It also greatly reduces the time the product needs to cool down for safe handling after the drying process.

Tenney designed this system to reside in a clean room and included a custom motorized material handling hand truck engineered to be an exact fit for the customer

This vacuum drying oven is designed to remove moisture from a large spacecraft engine after it goes through a washing process. (Courtesy: Tenney Environmental)

product. The hand truck allows one user to easily load and unload 800 pounds of product by themselves, which reduces risk of injury and labor costs.

"Our vacuum drying ovens are an extremely efficient way to remove moisture from almost any product faster and at lower temperatures than other conventional methods. This unit was customized to the customer's unique engine drying needs," said Rick Powell, vacuum products manager.

Features of this oven include:

› Control tolerance at sensor: ±5 torr.

› Pump capable of removing at least 3.5 pounds of water vapor per hour.

› 100°F to 140°F operating temperature range.

› On-board automated GN2 heater.

› 304 stainless steel interior.

MORE INFO www.tenney.com

Seco/Warwick wins third Innovation Leader award

Innovation Leader awards went to Seco/Warwick for the third time. The results of the company's work include numerous patented and award-winning technologies solving the problems of the heat-treatment industry. However, the company continues work on new, revolutionary projects.

The "Business Leader" event is a prestigious competition. The jury gives awards to the companies distinguished by their transparency and business honesty with innovative successes as their trademarks. Selected companies are awarded the prestigious Innovation Leader title.

Katarzyna Sawka, global group marketing director of Seco/Warwick, received the Innovation Leader Award on behalf of the company in October. She said, "We are proud of the solutions created by Seco/Warwick specialists. We do not stop long-term thinking and actions, which is the reason behind this drive towards new technologies in the heat-treatment industry 4.0. Labels such as 'leader,' 'trendsetter,' and 'champion' have been applied to Seco/Warwick around the world. Although it is a global opinion, we are happy that our company's efforts are recognized by industry juries. We believe it is important that Seco/Warwick creates such innovative solutions in the era of Industry 4.0."

The prefix "e" is common for the internet world. However, Seco/Warwick e-innovations are not a virtual creation but represent both e-conomical and e-nvironmentally friendly approaches to innovation. This philosophy enables it to be a leader both in business and in inventions.

This year, Seco/Warwick presented two innovations challenging the everyday problems of metal heat treatment: UCM® 4D Quench® and Super IQ®.

The UCM® 4D Quench® furnace is a modern alternative to press hardening and eliminates most of the dangers associated with the process. In turn, the Super IQ® system limits gas emissions and guarantees savings versus traditional furnaces.

"Our goal is to respond to the challenges faced by our customers from these very demanding industries. We have studied what improvements in terms of equipment operation can be introduced to broaden the purposes for which the furnaces can be used so we can deliver products that bring maximum benefits. This approach turned our premier systems — UCM® 4D Quench® and Super IQ® — into October's hit during expositions in the USA and Europe," said Sawomir Woniak, CEO, Seco/Warwick Group.

MORE INFO www.secowarwick.com

INDUSTRIAL HEATING EQUIPMENT ASSOCIATION

IHEA sets sail for 2020 Annual Meeting

Chief Master Sergeant (Retired) Bob Vazquez will present on SUPERvision!

The Industrial Heating Equipment Association is pleased to announce its 91st Annual Meeting will be on the high seas March 12-16, 2020, on Royal Caribbean's Brilliance of the Seas, departing from Tampa, Florida. IHEA has had several successful, high-quality annual meetings on cruise ships and is excited to offer this budget-friendly meeting to IHEA members once again.

This four-day event will feature two sea days and a day in Cozumel. As always, the annual meeting promises to deliver outstanding programming, committee work, and plenty of time for social interaction during the receptions and meal functions.

The program will include presentations from some of IHEA's past favorites: Chief Master Sergeant (Retired) Bob Vazquez, Chris Kuehl, and Omar Nashashibi.

Vazquez is a course director at the United States Air Force Academy's Center for Character Development, as well as an adjunct professor at the University of Colorado at Colorado Springs. He will be talking to us about the Power of SUPERvision. IHEA is happy to welcome him back after four years for his unique perspective on leadership.

Attendees will also hear from IHEA's economist Kuehl, who entertains as well as informs the crowd with his spirited delivery of the economic update.

With all eyes and ears on the capital, Washington, D.C. lobbyist Nashashibi will present an insider's perspective as the 2020 presidential election unfolds. As a bonus for all attendees, speakers will be available to continue discussions and answer questions in a more relaxed setting throughout the cruise.

IHEA committees will convene on board the Brilliance of the Seas to continue work on issues of importance to the membership and the industry at large. To round out the perfect meeting agenda, attendees will enjoy a variety of social activities including the sail away gathering, the welcome get together, the annual President's Reception, a mini-golf tournament, and the farewell dinner. The complete program and event details are available at www.ihea.org.

TRIP DETAILS

The four-night cruise will depart from Tampa on Thursday, March 12, and return to Tampa the following Monday morning, where guests will disembark to return home. As there are a variety of stateroom classes available onboard Brilliance of the Seas, IHEA has secured cabins in several different categories to provide cost flexibility to

The pool deck on Brilliance of the Seas is the perfect place to network between meetings during IHEA's 2020 Annual Meeting.

members. The cabin price is for one or two guests per cabin. There is no discount for a single passenger in a cabin.

The cruise fare, which is determined based on the cabin selected, includes:

› Ship accommodations for four nights.
› All meals onboard the ship.
› Deluxe drink package for the first and second person in each cabin (includes drinks up to $13 each).
› Access to all lounges, pools, and entertainment.
› Port taxes and fees.
› Gratuities.
› Onboard entertainment.
› IHEA Mini-Golf Tournament on the ship.

The Annual Meeting Registration Fee includes all committee meetings, general sessions, and evening receptions. Spouses/guests are welcome to attend the receptions at no charge.

Attire for the entire cruise is casual except for one evening called "Wear Your Best." This is a step up from casual but not formal. Our President's Reception will be that evening.

IHEA is excited to board Brilliance of the Seas, a mid-size ship that offers a great array of lounges, food options, and entertainment. At 91,000 gross tons, Brilliance of the Seas is the perfect size to balance a multitude of amenities with an intimate feel. The ship is built on the same hull as the Celebrity Constellation, which hosted IHEA's 2015 Annual Meeting. Reserve your cabin now and join us for IHEA's 91st Annual Meeting.

Don't miss the 2020 IHEA Annual Meeting, reserve your cabin now. www.ihea.org.

IHEA's 2020 Annual Meeting sets sail on board Brilliance of the Seas.

D. SCOTT MACKENZIE, PH.D., FASM
SENIOR RESEARCH SCIENTIST–METALLURGY /// QUAKER HOUGHTON INC.

Tramp elements of Ni, Cr, Mo, and Cu increase hardenability, but also increase the potential distortion of a part during heat treatment.

Hardenability – the influence of tramp elements

Hardenability is the property of a material to deeply harden, and not the ability to get hard [1]. This basic concept has driven much of the research in carbon and alloy steels since the 1920s. It is this concept that has enabled the development of high alloy steels such as SAE 4340 for high strength applications.

When the basics of hardenability were being developed, most steels were commonly produced by an open-hearth furnace, fed by a blast furnace. The molten steel was poured into ingots, where it was then hot-rolled, or forged into billets. Today, 65 percent of steel in the U.S, Japan, Europe, and Brazil is produced by electric arc furnaces, while in the rest of the world only about 35 percent of steel is produced in an electric arc furnace. The balance of the steel is produced by traditional blast furnaces and Basic Oxygen Furnace (BOF) [2]. The advantage of EAF technology, is that it allows nearly a complete charge of steel scrap, and can be turned off when not required due to market forces. Detailed specifications for the types of scrap to be safely used in electric arc furnaces have been developed [3]. Individual companies create individually tailored specifications.

Scrap steel is steel that has been recycled. At present, approximately 86 percent of steel is recycled [4]. This could be recycled cars, offal from cutting or shearing operations, or steel packaging. This steel scrap can be a mixture of different alloys and product forms. This means that instead of steel that contains only iron, carbon, silicon, and manganese, there may be tramp elements of nickel, chromium, and molybdenum.

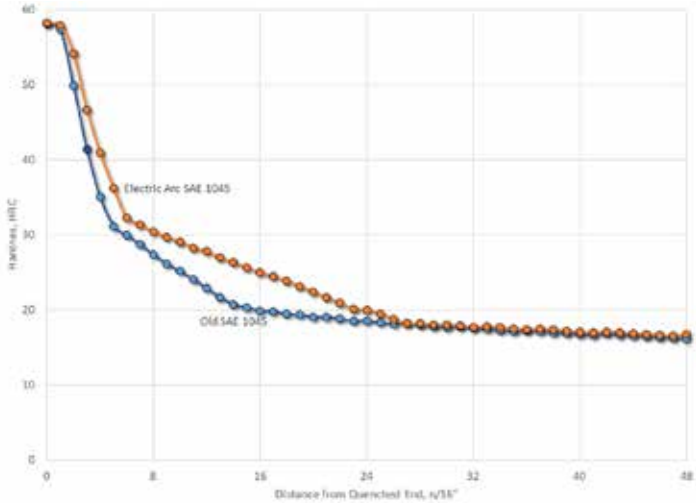

Figure 1. Calculated Jominy End Quench curves for two compositions.

	C	Mn	P	S	Si	Cr	Ni	Mo	Cu
Mid 1940	0.42	0.79	0.019	0.023	0.22	-	-	-	-
Today	0.42	0.79	0.019	0.023	0.22	0.11	0.18	0.04	0.04

Table 1. Comparison of the typical chemistries SAE 1045.

EFFECT OF TRAMP ELEMENTS ON HARDENABILITY

During the 1930s and '40s, when the concepts of hardenability were being developed, most steels were commonly produced in an open-hearth furnace, fed by a blast furnace. The simple steels like SAE 1045 only contained iron, carbon, silicon, and manganese. It is these

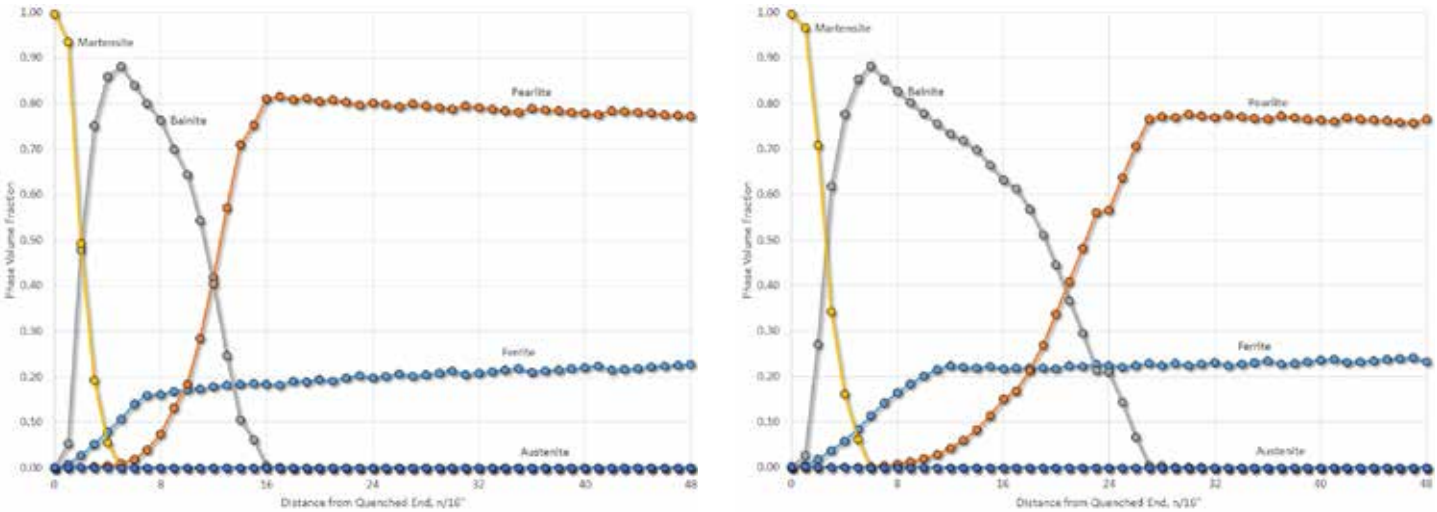

Figure 2. Comparison of the calculated phases present in an as-quenched Jominy End Quench bar, as a function of distance from the quenched end. Left graph is a traditional SAE 1045 with no tramp or residual elements. The right graph is from a modern SAE 1045 with limited residual elements.

Scrap steel is steel that has been recycled. At present, approximately 86 percent of steel is recycled. This could be recycled cars, offal from cutting or shearing operations, or steel packaging. This steel scrap can be a mixture of different alloys and product forms. (Courtesy: Shutterstock)

steels that many of the original Time-Temperature-Transformation and Continuous-Cooling-Transformation diagrams were developed. However, technology changed. More alloys are created using greater scrap content. This means that there are additional residual or tramp elements of nickel, chromium, and molybdenum now present in very simple steels. What is the impact of these residual elements on the hardenability of the steel? In this case, we examine two steels – one produced in the middle of the last century, and one that is produced today. The typical chemistries are shown in Table 1.

This assumes that both of these steels are fine-grained, with an ASTM grain size of 8. The amounts of additional tramp elements are very small – less than 0.4 percent. How likely are these elements to change heat-treatment response?

Using JMatPro [5], the Jominy curves of the two compositions shown in Table 1 were calculated. The results are shown in Figure 1.

As can be seen, the SAE 1045 with the minor amounts of tramp elements has a greater hardenability than the traditional SAE 1045. The transformed hardness of the modern SAE 1045 is much harder at all distances from the quenched end up to J=30.

Comparing the phases present along the length of the Jominy End Quench bar, the differences are more dramatic. In the traditional SAE 1045, the 50 percent martensite fraction occurs at J = 3, and pearlite tends to dominate at J = 12. In the SAE 1045 produced by an electric arc furnace, the 50 percent martensite fraction is at J = 3.5, and pearlite dominates at J = 21. There is a great deal more bainite in the modern 1045 than the traditional SAE 1045. This contributes to greater hardness, at greater depth. This comparison is shown in Figure 2.

Looking at the results of the Jominy End Quench, it can be seen

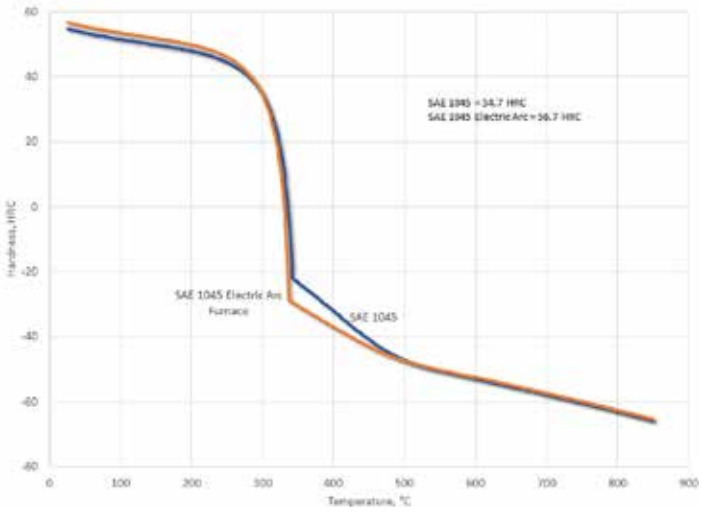

Figure 3. Comparison of two chemistries of SAE 1045 when quenched using a medium speed quench oil.

that there is a distinct difference in the response during quenching. How does this translate into the real world? Taking a medium speed, general purpose quench oil (Houghto-Quench G), with a moderate cooling curve, what would be the differences observed?

Using the "Quench Properties" of JMatPro, a specific time vs. temperature curve can be input, and the hardness and microstructures can be calculated. The results of these calculations are shown in Figure 3.

In Figure 3, it shows that the responses are similar. However, the

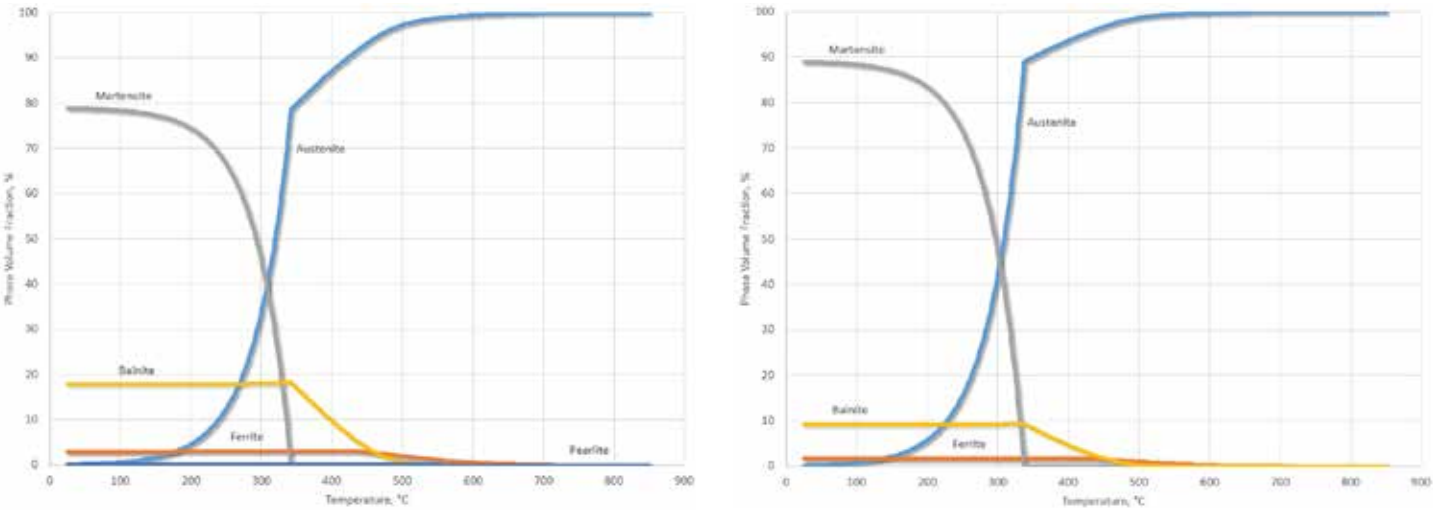

Figure 4. Comparison of phases present when quenching using a medium speed general purpose quench oil. Left graph is traditional SAE 1045 and the right graph is SAE 1045 with tramp elements present.

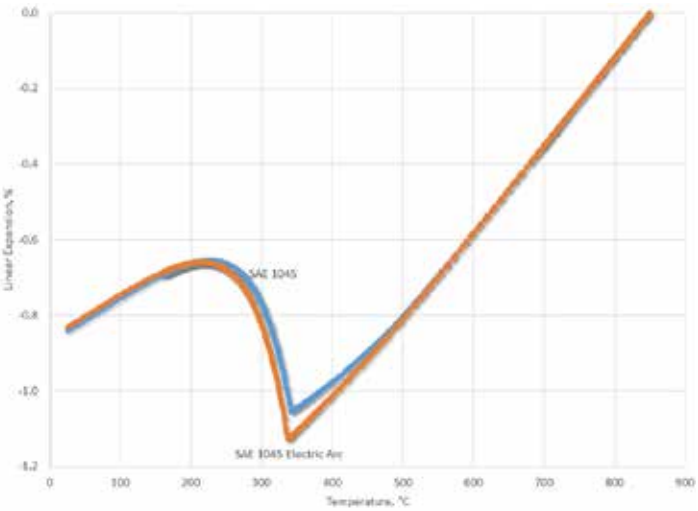

Figure 5. Calculated linear expansion of two chemistries of SAE 1045 steel after quenching with a medium speed, general purpose quench oil.

traditional SAE 1045 is 2 HRC softer at the surface than that of the electric arc furnace SAE 1045. This difference is small, but can be significant, for instance, when trying to achieve a specific case hardness during induction hardening, or when neutral hardening. The reason for the hardness difference is the fraction of phases present. In the case of the traditional SAE 1045, there is 79 percent martensite present, 18 percent bainite present, and approximately 3 percent ferrite present in the as-quenched microstructure. In the SAE 1045 EAF, there is 89 percent martensite present, 9 percent bainite present, and 2 percent ferrite present (Figure 4). This increased martensite fraction, when tempered to the same hardness, will achieve better fracture toughness than the traditional SAE 1045. In all, the EAF produced 1045 will have better response to heat treatment than a traditional SAE 1045.

From a distortion perspective, looking at the calculated linear expansion (similar to that measured by a Gleeble apparatus), the traditional SAE 1045 will exhibit less distortion during quenching than the EAF-produced SAE 1045 because of the lower fraction of martensite produced. There is a greater expansion during transformation to martensite (Figure 5). However, the end expansion is the same. Improvements in racking and fixturing are likely to be able to overcome these differences.

CONCLUSIONS

In this short discussion, the effect of tramp elements on the hardenability of a simple SAE 1045 has been shown. These tramp elements of Ni, Cr, Mo, and Cu increase the hardenability, but also increase the potential distortion of a part during heat treatment. These elements are due to the increased amount of scrap used in electric arc furnaces used for producing the dominant amounts of steel in the U.S., Europe and Japan.

Manufacturing is global. Identical parts can be produced at multiple locations around the globe. Steel is produced by many different methods, depending on the location. Developing countries such as China and India rely predominantly on blast furnace and BOF steels. It is these tramp elements that are missing in blast furnace and BOF steels that can explain the different response of identical parts process using the same manufacturing process, using ostensibly the same steel. Differences in heat treatment response and core hardnesses using the same grade of steel have to be understood and compensated for to achieve a consistent manufacturing product.

Should there be any questions regarding this article, or suggestions for further articles, please contact the editor or the author.

REFERENCES

[1] W. E. Jominy, Hardenability of Alloy Steels, Cleveland: American Society for Metals, 1939.

[2] T. Balcerek, "Turning Away From Blast Furnaces Still Leaves Problems for Steel Industry," 2015.

[3] Steel Dynamics, "Iron and Steel Steel Scrap Specifications Manual, Rev01," Columbus, OH, 2016.

[4] Steel Recycling Insistute, "Steel is the World's Most Recycled Material," 2017.

[5] Sente Software, "JMatPro," 11 November 2018. [Online]. Available: https://www.sentesoftware.co.uk/.

[6] M. Grossman, M. Asimow and S. F. Urban, "Hardenability, its Relation to Quenching and Some Qualitative Data in Hardenability of Alloy Steel.," 1938.

[7] L. Canale, J. Vatavuk and G. E. Totten, "Introduction to Steel Treatment," Comprehensive Materials Processing, vol. 12, pp. 3-37, 2014.

ABOUT THE AUTHOR

D. Scott MacKenzie, Ph.D., FASM, is senior research scientist-metallurgy at Quaker Houghton Inc. For more information, go to https://home.quakerhoughton.com/

JASON SCHULZE
METALLURGICAL ENGINEER /// CONRAD KACSIK

Proper procedures, careful records, and a thorough reading of the Nadcap guidelines make testing metallic materials a smooth process.

ASTM E18 and Nadcap: Rockwell hardness testing

Rockwell hardness testing is a common way to ensure the material response to heat treat is conforming and is required by applicable industry and prime specifications. Rockwell hardness testing is popular due to its ease of operation including the absence of optical measuring equipment, a range of alloys may be measured, and readings can be obtained in a matter of seconds with both manual and more modern automated machines.

ASTM E18 is the industry standard for Rockwell hardness testing of metallic materials. This specification includes both theory and standard practice statements. For those companies Nadcap accredited in heat treat where the AC7102/5 for hardness and conductivity testing is included, an additional layer of requirements come into play.

In this article we will examine general hardness testing theory, practices, Nadcap requirements, and discuss how these items affect those responsible for quality. The items within this article are general and, in an effort to manage the length of this article, not all aspects of hardness testing, ASTM E18, or Nadcap requirements are included. All references to ASTM E18 are to revision -19.

ROCKWELL HARDNESS TESTING THEORY

Rockwell hardness testing has several indenter types which in turn require separate major loads (kg). Figure 1 reflects common Rockwell scales used and their corresponding major loads.

When Rockwell hardness testing, a minor load of 10kg is applied to the indenter used on the material being tested. The purpose of the minor load is to penetrate the material's surface and establish a set position. After the minor load is applied, the major load is applied. Again, this major load is dependent on the type of indenter used. After enough time, the major load is removed and the hardness value is displayed on either an analog or digital indicator. Analog indicators typically have a resolution of 1 Rockwell while digital machines typically have an available resolution of 0.1 Rockwell.

The thickness of the material being tested should be taken into consideration. It is standard practice to ensure that the material being tested is 10x the indentation depth. Different Rockwell scales and the corresponding minimum hardness readings should be considered when identifying the thickness of the material. Figure 2 [1] reflects this comparison.

SURFACE PREPARATION

The surface intended for testing should be clean and somewhat smooth although grinding the material for hardness testing, especially on hardened materials, is not always a good practice. This type of surface preparation will cause the surface being tested to heat in that specific location and can reduce the hardness locally, making the readings less representative of the rest of the part. ASTM E18 requires the surface being tested be free of scale or oxides except in specified cases.

As with any test, the variables which increase error should be reduced as much as possible. Most testing procedures are established, and the practices repeated to ensure this occurs.

	ROCKWELL C	ROCKWELL A	ROCKWELL B
Major Load (kg)	150	60	100
Indenter	Brale	Brale	1/16th dia ball
Application	Hardened/ Tempered steel	Thin/hard materials such as W	Nonferrous steel, steel sheet, soft metals

Figure 1

	ROCKWELL SCALE		
Material Thickness "	C (150kg)	A (60kg)	B (100kg)
0.015	-	-	-
0.016	-	86	-
0.018	-	84	-
0.020	-	82	-
0.022	69	78	-
0.024	67	76	-
0.025	-	-	92
0.026	65	71	-
0.028	62	67	-
0.030	57	60	68
0.032	52	(a)	-
0.034	45	(a)	-
0.035	-	-	44
0.036	37	(a)	-
0.038	28	(a)	-
0.040	20	(a)	20

(a) - No minimum hardness for metal of ≥ thickness.

Figure 2

VERIFICATION TESTING

ASTM E18 lists three types of verification testing: direct verification, indirect verification, and daily verification. Direct verification is performed when the machine is purchased new from the manufacturer, when the indirect test fails, or when any adjustments, modifications or repairs have been made to the machine that could affect any testing variables. Indirect verification is performed annually, when a new machine is received and installed, or when a machine is moved. Daily verification is performed each day prior to using the hardness tester, when the anvil, test force, or indenter is changed.

The direct verification must be documented and available on-hand,

especially for those suppliers that are Nadcap accredited or seeking Nadcap accreditation. Nadcap heat treat auditor advisory HT-009 requires that the direct verification report for hardness testers included in the scope of the audit be on hand. If Nadcap suppliers do not have evidence the direction verification was performed, a finding may be issued. Quality staff should contact the manufacturer for a copy of the direct verification or send the machine to the manufacturer if evidence of direct verification is not on-hand.

Indirect verification is typically performed annually. This test should consist of the indenters used in production. Some suppliers ensure they have extra indenters available during the indirect verification process so that, if during production testing an indenter breaks and needs to be replaced, it can be replaced with an indenter that has been subject to the indirect verification process. It is also typical for indirect certifications to reflect maintenance performed per ASTM E18, although the supplier's internal procedure should state this is required during indirect verification. Something particular quality staff should verify when reviewing indirect verification certifications is reference to the correct revision of ASTM E18 at the time of calibration, as ASTM E18 has been revised 1-2 times per year for quite some time now.

Daily verification is performed prior to using the machine each day. Some suppliers choose to require (within their own internal procedures) that the daily verification be performed every eight hours. This is typically done when a supplier uses the hardness testing equipment frequently. While it is not required (only recommended) by ASTM E18 that daily verification results be documented, it is common practice for suppliers to document the daily verification results. When making a daily verification log, it may be in the supplier's interest to include additional items which will ensure conformance during audits. As an example, the supplier could include fields which show the indenter ID as well as the ambient temperature during tests. This would be evidence for auditors that, when the indenter is changed, a new daily verification test is performed. Figure 3 is an example of a daily verification log.

Hardness Test Machine;		Serial #:			Model #:			MFG:		
Date:	Operator:						Hardness Test Scale:			
		STD Value	STD Tolerance		Test 1	Test 2	Test 3	Error	Repeatability	Pass/Fail
Block ID:		32.5	±	1.0	32.6	32.3	32.2	-0.1	0.4	PASS
Block ID:		46.8	±	1.0	46.4	46.5	46.2	-0.4	0.3	PASS
Block ID:		61.2	±	0.5	60.6	61.1	61.0	-0.3	0.5	PASS
Testing per ASTM E-18		Indenter ID:					Test Temperature:			°F
Error = (Average of the 3 test values)-STD Value					*Repeatability = Highest Test Value-Lowest Test Value*					

Figure 3

It is typical practice for suppliers to verify the integrity of diamond indenters prior to daily verification through inspection, although this is not specifically required by ASTM E18 or the Nadcap checklist for hardness testing for the daily verification process. In fact, the only location within ASTM E18 that addresses inspection of diamond indenters is within Appendix A.3, paragraph A.3.5.2.1. This paragraph applies to the standardization of Rockwell indenters from the manufacturer, not the user (i.e. Nadcap accredited supplier). Although inspection of the diamond indenter is not required in either ASTM E18 or the Nadcap checklist for hardness testing, I have noticed findings being issued for the lack of an inspection prior to daily verification. This finding will typically be issued against ASTM E18 paragraph 5.4.1 which states, "Dust, dirt, or other foreign materials shall not be allowed to accumulate on the indenter, as this will affect the results." As you can see, this paragraph does not discuss the inspection of diamond indenters. If one was to keep the hardness tester covered between tests, this should suffice. The only specification that specifically requires the inspection of diamond indenters prior to daily verification is Boeings BAC5650. Regardless, findings seem to occur periodically for this and, therefore, it is recommended operators inspect indenters prior to performing the daily verification test.

NADCAP REQUIREMENTS

As with any Nadcap checklist, it is important to note when questions begin with the phrase, "do written procedures cover...". This is an indication that a supplier's written procedure must address each question that follows. As an example, AC7102/5(E), paragraph 2.7.1.1 asks "Do written procedures cover the number of test impressions for each test value reported?" This would require suppliers to document, within their written procedures, what each test value reported amounts to. Was it obtained from two values in the same area? Was it reported from a single value? Another is paragraph 2.7.1.4, which states "Do written procedures cover the locations for performing the tests?" This would require written procedures to state where to perform the hardness test in general or for each part/geometry tested.

Training is also something that should be addressed in detail. Operators performing hardness training are required to be trained on all geometries tested. This may include cylindrical parts which may require a correction as stated in Appendix A.6 of ASTM E18.

If hardness conversion is used, procedures should address the conversion method as well as the requirements of paragraph 3.5.3 of AC7102/5, which requires that hardness test reports show both the measure value as well as the converted value.

And last (but by no means least), suppliers need to ensure hardness indentations on hardness blocks are the proper distance from adjacent indentations as well as the edge of the hardness block used. This is a common finding in audits. Supplier's procedures should address the distance requirements but also state how to identify discarded indentations that are too close together or too close to the edge of the block.

SUMMARY

Hardness testing to ASTM E18 can be made simple once the proper procedures are in place and adequate training for operators and quality staff has been achieved. Quality staff should meticulously read through ASTM E18 as well as the Nadcap checklist (if it applies) to ensure all aspects of hardness testing are covered. Review of outside service certifications is a major part of this and should be designed into the quality system.

REFERENCE

[1] [1] ASM Metals Handbook, 1998, page 1312 Table 4.

ABOUT THE AUTHOR

Jason Schulze is the director of technical services at Conrad Kacsik Instrument Systems, Inc. As a metallurgical engineer with 20-plus years in aerospace, he assists potential and existing Nadcap suppliers in conformance as well as metallurgical consulting. He is contracted by eQualearn to teach multiple PRI courses, including pyrometry, RCCA, and Checklists Review for heat treat. Contact him at jschulze@kacsik.com.

COMBINING CLEANNESS, STRENGTH, AND TOUGHNESS FOR

AFFORDABLE POWER DENSIFICATION IN STEEL COMPONENTS

In order to facilitate increased gear-set durability or power density, ultra-high-strength, high-toughness, low-alloy steels are proposed.

By E. BUDDY DAMM

Increased power density in mechanical power transmission components means greater durability — allowing existing designs to achieve greater capacity or reduced size and mass for light weighting. After decades of work on adjusting gear-manufacturing practices, improving surface finishes, and changing designs to improve performance, trends are now turning toward a focus on improved performance with new gear-steel compositions and improved cleanness to enhance overall design.

Three new ultra-high-strength, high-toughness carburizable gear steels are introduced. The new steels provide yield strengths ranging from 180-210 KSI, ultimate tensile strengths ranging from 230-250 KSI, and Charpy impact energies ranging from 35 to 50 ft-lbf, allowing these grades to provide longer life, more power and/or lighter weight. The higher fatigue strength of these steels is compared to more commonly used gear steels, and an analysis is presented illustrating a potential for either a 30-percent reduction in gear set mass, or a 45-percent increase in gear-set torque capacity.

INTRODUCTION

Carburized gear steels are often the material of choice for mechanical power transmission systems requiring excellent power density. These steels commonly have a bulk carbon composition between 0.1 and 0.2 wt.%. The near surface is carburized such that the surface contains between 0.85 and 1 wt.% carbon. Carbon is diffused in to the surface creating a continuous gradient in carbon content between the surface and core carbon composition. The steepness of the gradient can be controlled through heat-treatment processes to provide the appropriate case-carbon profile for a given application. When properly quenched and tempered, this carbon gradient results in a hard surface needed to resist bending, rolling contact and sliding fatigue, and wear damage. The moderately strong but tough 0.1-0.2 wt.% carbon core provides resistance to core bending fatigue and overload fracture.

The gradient in carbon also plays a critical role in the evolution of residual stress during heat treatment. As a result of the carbon gradient, a compressive residual stress is generated on and near the surface, further enhancing fatigue performance. As the carbon content is increased, the temperature at which martensite forms is decreased. For every 0.1 wt.% increase in carbon content, there is a reduction in the martensite formation temperature of approximately 50°F [1]. As a result, during quenching of a carburized gear, the transformation of the near surface layer is delayed to a lower temperature than the core. When martensite forms from austenite, there is a 1- to 4-percent volume expansion [2][3] (increasing with the carbon content). When the lower carbon core transforms first, the austenitic material in the case is able to accommodate the expansion through plastic deformation. Moments later, when the case transforms to martensite, the hardened martensitic core does not yield. The volume expansion

Steel	Temper Temperature	Yield Strength	Ultimate Tensile Strength	Elongation	Hardness	Fracture Toughness, K_{IC}	Charpy Impact 72°F	RRMoore Fatigue Strength	Fatigue Strength
Units	°F	KSI	KSI	%	HRC	KSI-in$^{0.5}$	ft-lbf	KSI	KSI
9310	300	155	175	16	37	85	25	-	88
9310	500	137	165	16	36	137	65	-	83
4820	400	120	154	15	30	93	30	-	77
8620	300	157	199	13	42	64	14	-	100
3310	350	159	193	16	40	114	45	-	97
18CrNiMo7-6	400	130	175	15	38	105	38	105	88
Red Cells are calculations as shown in this row for each column						$(290*RTIE)^{0.5}$	$(K_{IC})^2/290$		UTS/2

Table 1: Nominal mechanical properties for some commonly used carburizing gear steels.

Steel	Temper Temperature	Yield Strength	Ultimate Tensile Strength	Elongation	Hardness	Fracture Toughness, K_{IC}	Charpy Impact 72°F	RRMoore Fatigue Strength	Fatigue Strength
Units	°F	KSI	KSI	%	HRC	KSI-in$^{0.5}$	ft-lbf	KSI	KSI
Ferrium C61	900	225	240	16	49	130	40	-	120
Ferrium C64	925	199	229	18	49	85	17	-	115
Pyrowear 675	600	143	185	20	40	150	53	-	93
Pyrowear 675	950	154	185	20	39	125	37	-	93
Red Cells are calculations as shown in this row for each column							$(K_{IC})^2/425$		UTS/2

Table 2: Nominal mechanical properties for some specialty carburizing gear steels used primarily in military aerospace applications where the potential for high temperatures exist.

Steel	Temper Temperature	Yield Strength	Ultimate Tensile Strength	Elongation	Hardness	Fracture Toughness, K_{IC}	Charpy Impact 72°F	RRMoore Fatigue Strength	Fatigue Strength
Units	°F	KSI	KSI	%	HRC	KSI-in$^{0.5}$	ft-lbf	KSI	KSI
EN27	400	177	225	15	42	108	35	-	113
4333MV	400	202	258	13	46	91	20	-	129
EN30B	400	199	247	12	45	69	22	-	123
HS220-27	400	198	249	18	45	83	34	-	125
Red Cells are calculations as shown in this row for each column									UTS/2

Table 3: Nominal mechanical properties for some ultra-high-strength alloy steels with good toughness and the potential to be carburized.

in the case now results in the formation of a compressive residual stress profile near the surface. In order to optimize the evolution of compressive residual stress, a carbon gradient and associated martensite start gradient are necessary.

Increasing the carbon content of steels, when fully and properly hardened, results in higher strength, but with increased strength comes decreased toughness. These competing factors create a challenge for the gear-steel designer. In order to improve gear performance, both higher core strength and toughness are needed, as is compressive residual stress. Core carbon content has the single greatest effect on core strength and is, hence, a natural place to start toward improving gear performance. Careful use of other alloying elements is then needed to help maintain or even improve core toughness. Consideration must also be given to the evolution of residual stress and the effect of the core carbon content. The increase in core carbon content results in a decrease in the compressive residual stress. Here, the key is to only increase the core carbon content enough such that the credit gained in core strength is not offset by the debit given in residual stress.

Steel	Temper Temperature	Yield Strength	Tensile Strength	Elongation	Charpy Impact Energy (room temp., Long.)	K1C Fracture Toughness	Pass/Fail	designation
Units	°F	KSI	KSI	%	ft-lbf	KSI root in.		
Aims		180+	220+	-	40+	90+	-	
Alloy 1	400	185	230	14	49	115	Pass	UHS230-47
Alloy 2	400	208	246	13	30		Fail	
Alloy 3	400	187	237	12	17		Fail	
Alloy 4	400	187	232	14	50	108	Pass	UHS230-44
Alloy 5	400	197	241	13	38		Fail	
Alloy 6	400	187	235	12	35		Fail	
Alloy 7	550	212	254	12	32	97	Fail	
Alloy 8	930	187	241	13	20	83	Fail	
Alloy 9	400	210	250	12	41	110	Pass	UHS250-35
Alloy 9	930	176	187	17	47		Fail	

Table 4: Tensile and room temperature Charpy impact energy values for the nine initially designed steel chemistries studied.

Steel	Temper Temperature	Yield Strength	Ultimate Tensile Strength	Elong.	Hardness	Fracture Toughness, K_{IC}	Charpy Impact 72°F	Charpy Impact -49°F	RRMoore Fatigue Strength	Aprx. Fatigue Strength
Units	°F	KSI	KSI	%	HRC	KSI-in$^{0.5}$	ft-lbf	ft-lbf	KSI	KSI
UHS250-35	400	214	253	14	48	110	38	37	113	127
UHS250-35	600	207	231	13	46	-	37	20	-	115
UHS230-44	400	185	230	14	44	108	50	42	-	115
UHS230-47	400	190	230	15	48	115	39	34	107	115
UHS230-47	600	178	210	15	44	-	34	22	-	105
Red Cells are calculations as shown in this row for each column										UTS/2

Table 5: Nominal mechanical properties for TimkenSteel's new ultra-high-strength, high-toughness carburizable gear steels.

Tables 1 to 3 show some nominal mechanical properties for existing and potential gear steels. Yield strength tends to correlate with fatigue initiation, while hardness and ultimate tensile strength tend to correlate better with fatigue strength. The last two columns show the calculated fatigue strength estimated as half of the UTS, and as a function for Rockwell C hardness respectively [4]. Charpy impact values and fracture toughness values are weakly correlated and are shown near the middle of the tables. If measured RR Moore rotating bending fatigue data is available, those data are shown as well. In all cases, values shown in red are calculated values using the equations shown at the bottom of each column.

Table 1 shows nominal properties of some commonly used carburized gear steels when tempered between 300 and 500°F. Strength, Charpy impact energy, and fatigue strength values are varied, but nominal values of 130 KSI yield, 175 KSI UTS, and 80 KSI for fatigue strength are representative for this class of gear steels. Charpy impact values range from 15 to 65 ft-lbf and are inversely correlated to strength. At the nominal strength levels noted, the nominal impact energy is 30 ft-lbf.

Table 2 shows nominal properties for some specialty alloys designed for use in military and aerospace applications where potential oil-out conditions exist. Here the need to escape danger while there is no remaining oil drives the need for high-temperature retention of surface hardness, core strength, and toughness. These performance capabilities are impressive, but come at a price point of 10 to 10s of dollars per pound, and so are included here as comparable examples. The remaining steels described in this manuscript, including the new ultra-high-strength, high toughness steels fall in to a price point of 1 to a few dollars per pound.

Table 3 shows the nominal properties of some ultra-high-strength steels tempered at 400°F. For these steels, the nominal carbon contents range between 0.24 and 0.34 wt.%. This carbon level falls within the range expected to provide good carburizing and residual stress response and yields increased core strength and fatigue capabilities. Here, nominal values for yield and UTS are approximately 180 and 230 KSI respectively with expected fatigue strength of 115 KSI. For these steels, the increase in strength comes at the cost of Charpy impact toughness in the range of 20 to 35 ft-lbf. While the strength and concomitant fatigue strengths are improved compared to commonly used gear steels shown in Table 1, the Charpy impact values are only on par with commonly used gear steels.

Making changes from common carburized gear alloys to new alloys consumes time, resources, and dollars. In order to justify pursuing gear steel material changes objectives of a 25-percent increase in tensile and fatigue strength, in combination with a 25-percent increase in Charpy impact energy values were targeted in developing the new steels described below. Design minimum target values of:

- 180 KSI YS,
- 220 KSI UTS,
- 110 KSI fatigue strength, and
- 40 ft-lbf Charpy impact energy (room temperature, longitudinal)

were selected.

Previous publications have described how improvements in clean-steel technology have driven the ability to provide design relevant cleanness metrics to gear designers [5]. These technologies provide affordable solutions for critical, power-dense components. The clean steels technology combines advanced electric arc melting, vacuum ladle refining and teaming practices with advanced automated scanning electron microscope (SEM)-based steel cleanness evaluation. The result is certified ultra-clean steels on par with re-melted steel

and with cleanness metrics that are relevant to component design life. As strength is increased, steel cleanness becomes more critical. Steel cleanness is a critical enabling technology to fully realize the potential gains associated with these new ultra-high-strength, high-toughness steels.

DEVELOPMENT OF NEW ULTRA-HIGH-STRENGTH, HIGH-TOUGHNESS GEAR STEELS

A series of eight alloy steels were designed based on several factors, including a review of existing and incumbent gear and ultra-high-strength alloys, literature and patented steels, and computational thermodynamic assessment. An additional ninth alloy from a production chemistry was also included. At the time of writing this manuscript, the top-performing alloys from the test matrix have been submitted for patenting, and hence it is not possible to share full details of the chemical compositions studied. A target carbon content range of 0.24 to 0.30 wt% was selected. Carbon is necessary for strengthening, but excess carbon results in lower toughness and less favorable compressive residual stress profiles in the carburized case. The balance of other alloying elements studied for each variant were selected to optimize heat-treatment processes to maximize toughness at the target strength levels.

Six of the designed alloys aimed to achieve optimal strength and toughness when quenched and tempered at 400°F, one was designed to be quenched-and-tempered at 550°F, one was designed to be quenched and secondary hardened at 930°F, and one alloy was selected for either a quench-and-temper at 400°F, or quench and secondary harden at 930°F; 100-pound heats were produced via a laboratory scale vacuum induction melting facility using electrolytic iron and high purity alloy additions.

Residual elements such as P, Sn, and S were intentionally added at levels that simulate production levels typically achieved in electric arc furnace melted and vacuum refined steels. The 5.5" diameter ingots were forged to 2.5" square bars (reduction ratio = 3.8:1), and sample coupons were sectioned for heat treatment and mechanical testing. Coupons were normalized, quenched and tempered, or secondary hardened at and near the design optimal temperatures. Table 4 summarizes the tensile and Charpy impact properties generated from the test matrix. Three of the nine alloys met the design minimums for strength and Charpy impact energy and were down selected, provided designations as shown in the table, and prepared for further evaluation.

Table 5 shows additional data for the three down-selected alloys. KIC fracture toughness, -49°F Charpy impact, and U-notched rotating bending fatigue data were generated for these alloy and heat-treat conditions. Comparing these data to the incumbent carburized gear steel data shown in Table 1 shows significant improvements were achieved. Figure 1 shows yield strength vs. impact energy for incumbent alloys vs. these new ultra-high-strength, high-toughness steels. Figure 2 shows KIC fracture toughness plotted against room temperature longitudinal Charpy V-notch impact energy for this study.

The alloys used to generate these data are those alloys shown in Tables 3 to 5. It was observed that when tempering at lower temperatures (400-550°F) the data trended differently than when tempered above 600°F. The relationships between fracture toughness and Charpy impact shown in Figure 2 are those used in Tables 1 and 2.

Standard 120-ton production heats of UHS230-47 and UHS250-35 have been produced, and 3.75", 5.5", 11", and 13" bars have been hot rolled. Two heats of UHS230-44 were produced in the fall of 2018. Some of the material has been sold for initial manufacture of new products; some has been supplied to customers for trials and tests, and some remains available. Early results indicate that

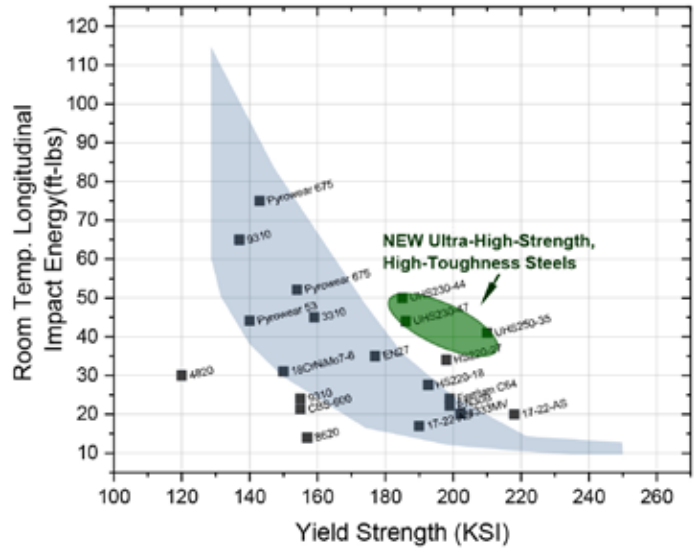

Figure 1: Yield strength vs. room temperature longitudinal Charpy impact energy absorbed for a range of existing and potential carburized gear steels. The new TimkenSteel ultra-high- strength, high-toughness steels are shown in the green oval.

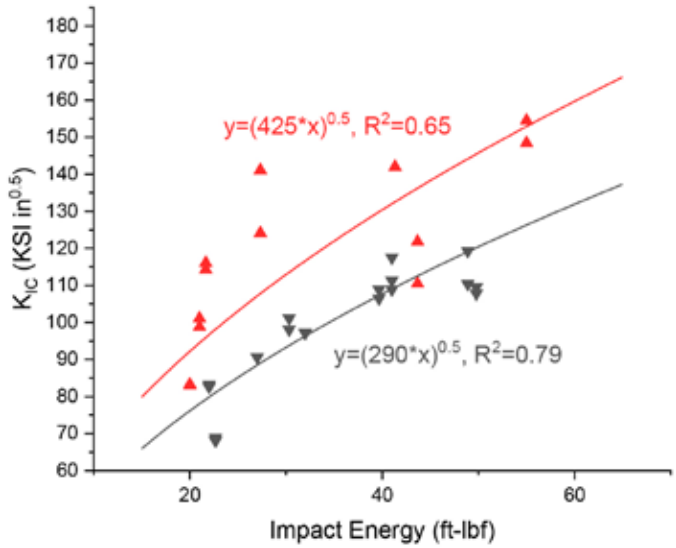

Figure 2: Observed relationship between KIC fracture toughness and room temperature longitudinal Charpy v-notch impact toughness. The black data represent conditions tempered between 400 and 550°F, and the red for 600°F and above.

UHS230-47 samples are meeting requirements in section sizes up to 10", and UHS250-35 samples are meeting requirements in section sizes up to 2.5".

COMPARATIVE CARBURIZATION EVALUATION

A carburization trial was performed on the new alloys and some commonly used carburized gear steels in order to develop some baseline data on the carburizing behavior of the new alloys. Steel grades 9310, 4320, and 8620 were selected for comparison. Coupons measuring 1/2" thick, 1" by 2.5" were prepared with the 1" by 2.5" face on the longitudinal rolling direction plane. The samples were carburized at 1,700°F for 4.5 hours with a 1-percent carbon potential, furnace cooled to 1,500°F and held for 0.5 hours using a 0.85-percent carbon potential, and quenched in room-temperature oil. Sets of each alloy type were tempered at 400°F and a set of the new alloys and 9310 were tempered at 600°F. These carburization data are presented as

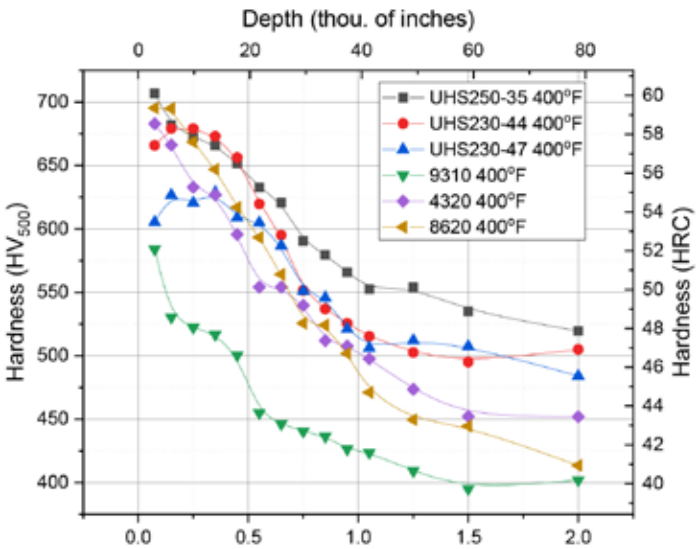

Figure 3: Case hardness profiles for samples tempered at 400°F.

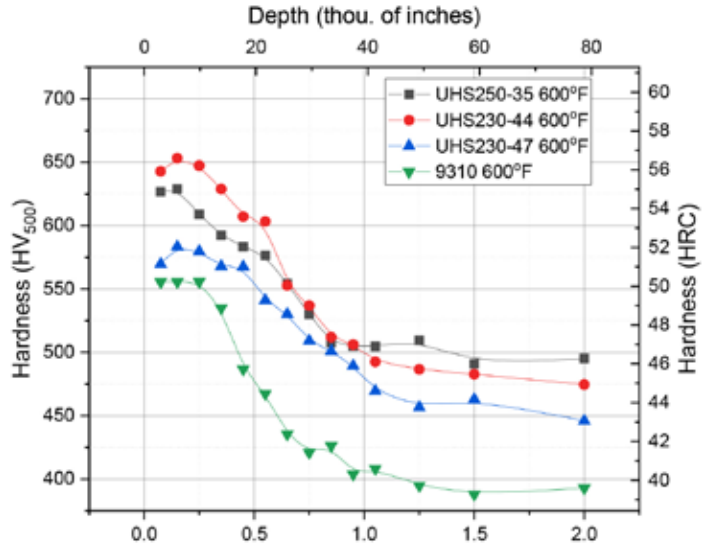

Figure 4: Case hardness profiles for samples tempered at 600°F.

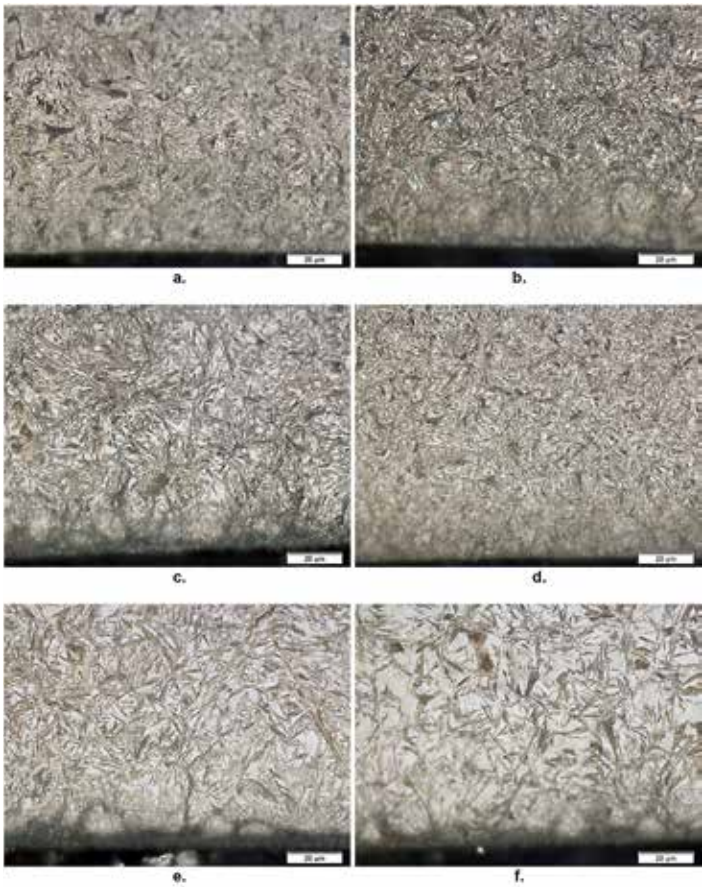

Figure 5: Near-surface microstructure of carburized and 400°F tempered samples: a) 4320, b) 8620, c) 9310, d) UHS250-35, e) UHS230-44, f) UHS230-47

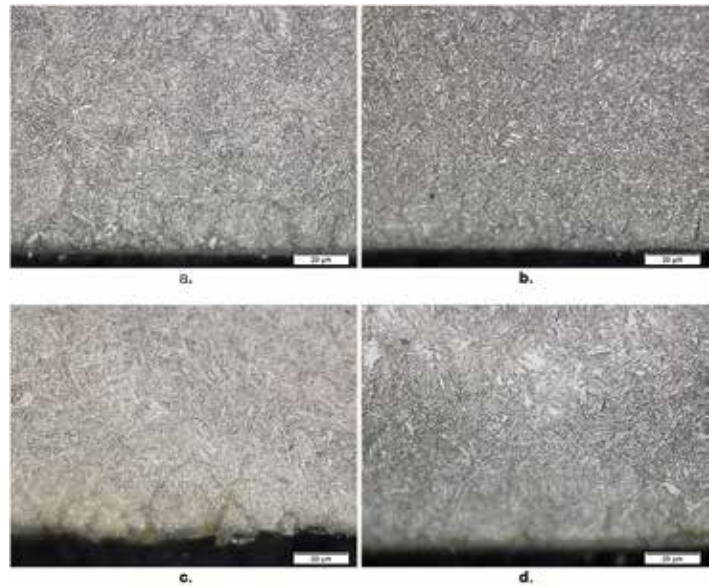

Figure 6: Near surface microstructure of carburized and 600°F tempered samples: a) 9310, b) UHS250-35, c) UHS230-44, d) UHS230-47.

baseline data. Implementation of any new gear steel into a given supply chain or process path will require development efforts to optimize the new alloy.

When tempered at 400°F (see Figures 3 and 5), UHS250-35 and UHS230-44 exhibited similar surface hardness as 4320 and 8620 steels, a deeper case depth to HRC 50, and a higher core hardness.

UHS230-47 exhibited a lower surface hardness compared to the other UHS-HT steels, but a higher surface hardness compared to 9310 steel. UHS230-47 exhibited deeper case depth to HRC 50 and higher core hardness compared to the common gear steels. Micrographs of the carburized structure are shown in Figure 5. The UHS230-44 alloy exhibits a slightly higher degree of grain boundary oxidation, which should be mitigated by either low pressure gas carburization, or post carburization grinding.

UHS230-47 exhibits more retained austenite near the surface which is most likely the reason this alloy exhibits a slightly lower surface hardness then the others.

When tempered at 600°F (see Figures 4 and 6), UHS250-35 and UHS230-44 exhibited similar surface hardness to each other and a deeper case depth to HRC 50 than UHS230-47. Grade 9310 exhibits the lowest hardness profile and core hardness.

POWER DENSIFICATION EXAMPLES

Power Densification through Higher-Strength, Tough Steels

In order to assess the magnitude of the potential for either light-weighting or increased power throughput, the effects of traditional vs. ultra-high-strength, high-toughness gear steels on gear set design were assessed. The Technical Resource "ANSI/AGMA 2001-D04,

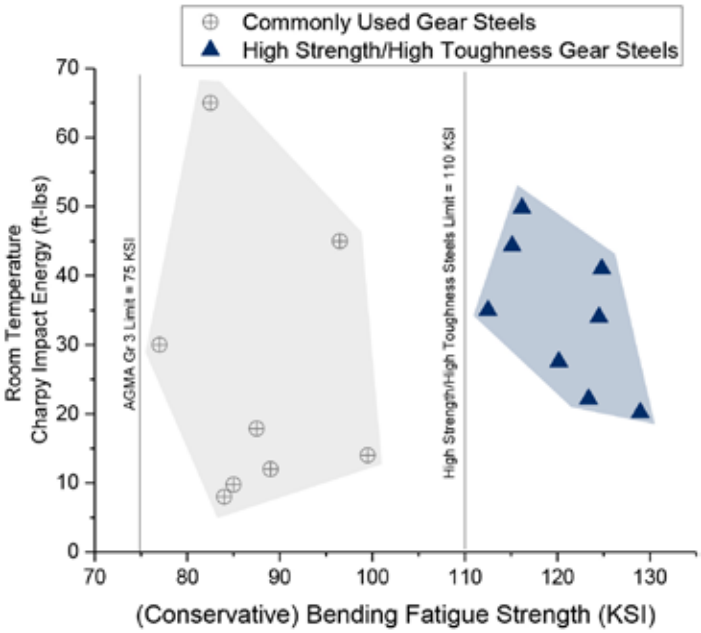

Figure 7: Area charts demonstrating the range of fatigue strength and Charpy impact energy (toughness) combinations achieved with typical (8620, 3310, 4820, 4620, 9310) gear steels (gray shading) and affordable, patent pending, ultra-high-strength, high-toughness steels for gears (blue shading). The vertical lines represent the fatigue strength used to compare these two alloy types below.

Fundamental Rating Factors and Calculation Methods for Involute Spur and Helical Gear Teeth" [6] provides a framework and the equations necessary to make such estimates. In Table 4 of this AGMA resource, the allowable bending stress for grade 3 carburized and hardened gears is listed at 75 KSI. This value is also shown as the AGMA limit in Figures 7-9. The allowable limit for high-strength, high-toughness steels is also shown in Figures 7-9 at 110 KSI. In each case, for traditional and for high-strength, high-toughness gear steels, the actual fatigue capacity may be measurably higher than these conservative limits and will be further dependent on the steel grade and heat-treatment processes selected. For the sake of illustration, the bending stress fatigue limits of 75 KSI and 110 KSI were selected for further calculations.

A generic pinion-and-gear set was conceived, and the calculations for this gear set were built in a spreadsheet in order to assess the magnitude of potential benefits. Figures 7 and 8 show the results of these calculations. The switch from commonly used gear steels to high-strength, high-toughness gear steels can result in a 45-percent horsepower increase. Alternatively, a 30-percent weight reduction with the same horsepower can be achieved. When a gear set design requires higher performance, high-strength, high toughness gear steels help meet the objective.

FUTURE WORK

Implementation of these new ultra-high-strength, high-toughness alloys into gearing applications is likely to follow two paths: In many cases, gear makers and users are looking for solutions to solve existing service life or design limitations. In these cases, implementation can occur on a case-by-case basis with the necessary engineering and design rigor to assure confidence in implementing these new alloys. In order to proliferate these new alloys in to gearing systems at a higher rate, AGMA and ISO standards should be updated. For gearing steel, AGMA 923 [7] a grade level 4 is proposed, which should

In order to facilitate increased gear-set durability or power density, ultra-high-strength high-toughness, low-alloy steels are proposed.

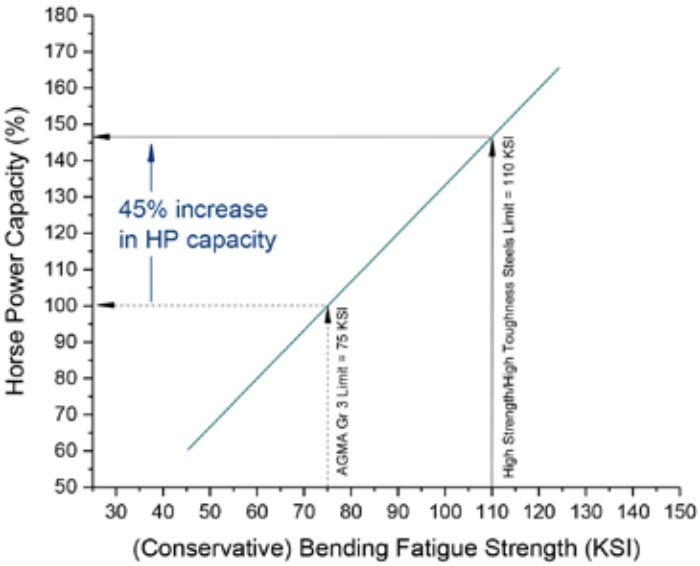

Figure 8: Assuming an increase in fatigue strength from 75 to 110 KSI results in a 45-percent increase in gear set horsepower capacity. Relative horsepower capacity (as a percentage) as a function of the bending fatigue strength calculated per the AGMA 2001-D04 technical resource.

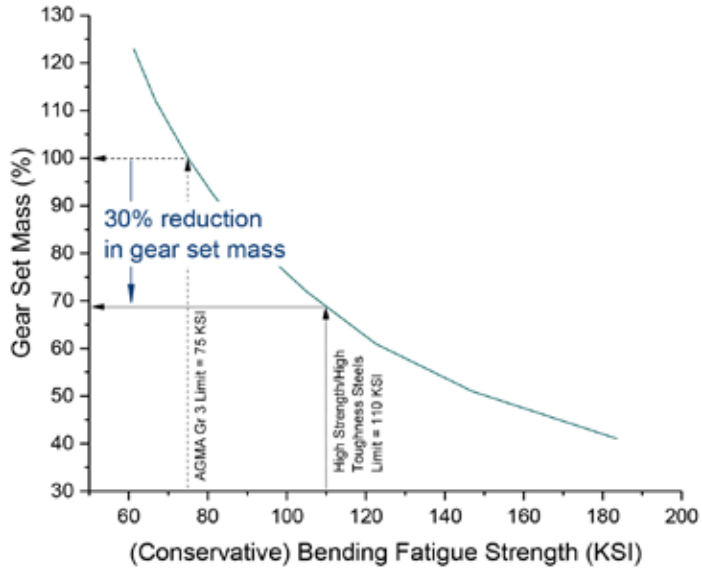

Figure 9: Assuming an increase in fatigue strength from 75 to 110 KSI results in a 30-percent reduction in gear set mass. Relative gear set mass (as a percentage) as a function of the bending fatigue strength calculated per the AGMA 2001-D04 technical resource.

	Yield Strength (KSI)	Ultimate Tensile Strength (KSI)	Charpy Impact (ft-lbf)	Fatigue run-out strength (KSI)
Common Gear Steels	130	175	30	80
New Ultra-High Strength, High Toughness Steels	190	230	40	110
% improvement	46%	31%	33%	38%

Table 6: Nominal properties and % improvement between common gear steels and the proposed new alloys.

include improved cleanness standards as described previously [5]. For gear capacity rating ANSI/AGMA 2004 [6], an increased root bending fatigue limit of 110 KSI is proposed for grade 4 steels with an ultimate tensile strength of 220 KSI or higher.

SUMMARY AND CONCLUSIONS

In order to facilitate increased gear-set durability or power density, ultra-high-strength high-toughness, low-alloy steels are proposed. Further, since implementation of new gear alloys is costly and time-consuming, a minimum improvement of 25 percent was targeted. Table 6 shows the improvement achieved in strength, toughness, and fatigue performance are between 30 and 45 percent. The improvement in mechanical properties and their effects on gear rating were assessed using the ANSI/AGMA 2001-D04 standard. For the example chosen, a 30-percent decrease in gear set mass, or a 45-percent increase in horsepower capacity are predicted.

BIBLIOGRAPHY

[1] G. Krauss, 2005, Steels: Processing, Structure and Performance, 3rd ed., Table 5.1.

[2] J. M. Moyer, G. S. Ansell, "The Volume Expansion Accompanying the Martensite Transformation in Iron-Carbon Alloys", 1975, Met. Trans. A, V6A, pp 1785-1791.

[3] L. Cheng, A. Böttger, T. H. de Keijser, E. J. Mittemeijer, "Lattice parameters of iron-carbon and iron- nitrogen martensites and austenites", Scripta Metallurgica et Materialia, Volume 24, Issue 3, March 1990, Pages 509-514,

[4] Murikami, T., 2002, Metal Fatigue: Effects of Small Defects and Nonmetallic Inclusions, 1st ed., Elsevier, London.

[5] E. B. Damm, P. C. Glaws, "Gear Design Relevant Cleanness Metrics", 2016, AGMA FTM.

[6] ANSI/AGMA 2001-D04, "Fundamental Rating Factors and Calculation Methods for Involute Spur and Helical Gear Teeth", 2004.

[7] AGMA 923-B05 "Metallurgical Specifications for Steel Gearing," 2005.

ABOUT THE AUTHOR

E. Buddy Damm is a steel solutions scientist at TimkenSteel Corporation and is responsible for developing new or improved products for TimkenSteel's customers and developing new or improved processes for TimkenSteel's manufacturing operations. In his 20-year tenure, he has served as a research and development engineer, failure analyst, and engineering manager. He has expertise in Integrated Computational Materials Engineering (ICME), thermodynamics, and kinetics of microstructure evolution, thermo-mechanical processing, fatigue and fracture mechanics, and failure analysis. Damm holds a bachelor's degree in metallurgical engineering from Michigan Technological University and a master's degree and doctorate in material science and engineering from Colorado School of Mines. He can be reached at e.buddy.damm@timkensteel.com.

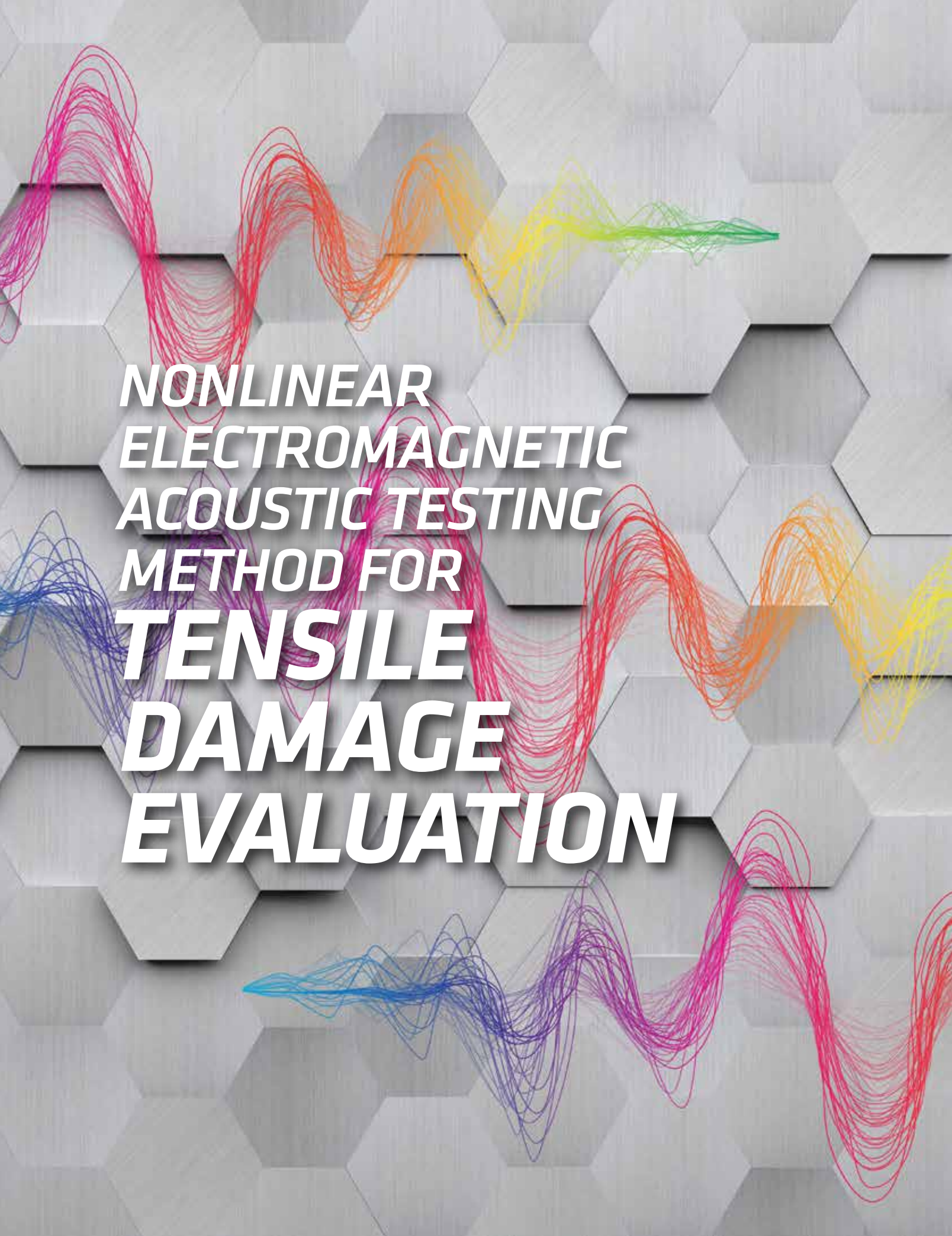

NONLINEAR ELECTROMAGNETIC ACOUSTIC TESTING METHOD FOR TENSILE DAMAGE EVALUATION

Tensile damage behavior of a nonlinear longitudinal wave is investigated, and from an experimental perspective, this research demonstrates the feasibility and robustness of the noncontact EMAT method for nonlinearity measurement with a longitudinal wave.

By ZHICHAO CAI, HAO CHENG, and CHENGCHENG LIU

This paper describes an approach for measuring material plasticity using contactless electromagnetic acoustic method. Harmonic generation from noncumulative fundamental longitudinal wave in specimen is studied based on numerical method, and the contribution to harmonic generation from tensile damage is shown to be higher than that from a geometric factor; more serious damages increase the amplitude of second harmonics. These two experimental setups (nonlinear piezoelectric method and nonlinear electromagnetic acoustic method) are used to assess the relative nonlinearity parameters of tensile damage of five aluminum alloy specimens along the thickness direction, and the proposed technique is as effective with the traditional nonlinear piezoelectric method. This result demonstrates that the ultrasonic nonlinear parameter can represent tensile damage with ultrasonic nonlinear parameter by noncontact electromagnetic acoustic method.

1. INTRODUCTION

The application of ultrasonic waves in engineering structure now is a critically significant method in nondestructive testing (NDT) and structural health monitoring (SHM). With the latest developments in image processing and mathematical and computer modeling, more sensitive and economical ways of looking at materials and structures have become possible when compared to the other inspection techniques [1]. The traditional ultrasonic testing method is based on the linear theory and depends on measuring particular parameters, including the size, the orientation, the location of crack, the acoustic velocity, the attenuation, and the transmission and reflection of ultrasonic wave to detect damage [2]. However, traditional linear ultrasonic methods detect cracks or features based on the order of the wavelength of the ultrasonic wave. They are sensitive to microstructural features that are orders of magnitude bigger than the wavelength, but linear ultrasonic testing is not sensitive to early-stage degradation and microcrack of materials without diffraction and attenuation effect. Therefore, the detection of early damage becomes an issue and advanced ultrasonic testing becomes strongly needed. In addition, the development of the ultrasonic testing method is a challenging task that should have several crucial applicative functions such as online evaluation, condition-based maintenance, fitness determination for service and remaining useful time, less cost and labor, required baseline, and required environmental data compensation methods. The nonlinear ultrasonic method has a powerful ability to characterize microstructural features in materials. The basic physical mechanism of higher harmonic generation, subharmonic generation, shift of resonance frequency, and mixed frequency response are introduced with applications to evaluation of microdamage. These effects are quantified with the measured acoustic nonlinearity parameter (ANP), which is caused by the interaction of a sinusoidal wave and microstructural features such as microcracks, precipitates, creep, fatigue, and plasticity [3–8] (i.e., features at the micron scale and below), and the ANP is a powerful indicator of the material state.

Currently, a number of investigators have applied nonlinear ultrasonic techniques to assess the damage in different metallic alloys such as early fatigue damage in Ti-6Al-4V specimens [9], heat-treated Cr-Mo-V steel [10], hardening in ASTM A710 steel [11], nickel-based superalloy samples under monotonic and fatigue loading [12], and plastic deformation in AL 1100-H16 alloy [13]. It is noted that the ANP, which is based on the fundamental and second harmonics, significantly changes with the damage.

The most commonly used nonlinear wave technique uses through-transmission bulk waves, which is applied in the field since access to both sides of the specimen is required. Longitudinal waves have the advantage, as compared to shear waves [14], of transferring energy to second harmonics; shear waves transfer energy to third harmonics. Therefore, it is more possible for nonlinear longitudinal wave to assess the material inner damage. In addition, nonlinear Rayleigh surface and Lamb waves are widely used to represent the material superficial or integral damage, which, with a smaller diffraction and attenuation, effects with long distance traveling.

However, most nonlinear ultrasonic applications detect material characterization and the existence of minute defects by piezoelectric ultrasonic method and a high nonlinear efficiency of a liquid coupling medium. The piezoelectric ultrasonic method is not appropriate for testing in extreme conditions and rough testing surfaces, and coupling medium affects the scan efficiency of the specimen to be measured. Therefore, noncontact ultrasonic testing method has a better application prospect. Sebastian et al. present noncontact an air-coupled ultrasonic technique for a nonlinear Rayleigh surface wave measurement of the relative nonlinearity parameters of two aluminum alloy specimens AL2024-T351 and AL 7075-T651 [15], but the ultrasonic conversion efficiency is not enough with the acoustic impedance mismatch. A study of Liu et al. makes use of the nonlinear laser ultrasonic method to perform fatigue crack measurements [16]. However, the laser ultrasonic method suffers from variations in optical reflectivity and is only feasible for specimens with highly reflective surfaces.

An electromagnetic acoustic transducer (EMAT) is a kind of sensor that can excite and receive ultrasonic waves without coupling agent. The EMAT can be designed to generate and measure the desired mode of elastic waves on the basis of the contactless coupling mechanisms. Various propagation modes can then be used to meet

a wide range of measurement needs, like the SH mode only being available with the EMAT technique; this is one of the advantages over the air-coupled ultrasonic technique and laser ultrasonic technique [17, 18]. The axial shear wave on cylindrical Cr-Mo-V specimens was found to be capable of fatigue and creep deformation of the nonlinearity measurement under the magnetostriction-type EMAT exciting [19, 20]. Cobb et al. present an approach of acoustic nonlinearity of fatigue damage accumulation that uses Rayleigh waves generated from EMAT and electromagnetic acoustic resonance [21, 22]. With the optimization of a pulse current generator [23, 24], EMAT has succeeded to excite vibration amplitude in the material high enough to induct higher harmonics, and the EMAT has the potential study in the nonlinearity measurement to isolate materials' nonlinearity. The objective of the current study is to explore the feasibility of a noncontact, electromagnetic acoustic technique to assess the acoustic nonlinearity parameter using nonlinear longitudinal waves. Section 2 presents nonlinear mechanics preliminaries based on the Murnaghan model. Section 3 presents the nonlinear characteristic obtained from numerical simulations. The two nonlinear ultrasonic methods are compared and analyzed in Section 4 and Section 5, respectively. Finally, conclusions are drawn in Section 6.

2. PRINCIPLE

The principle of the electromagnetic-acoustic coupling process is the elastic response to periodic surface stresses that arise from Lorentz forces. An alternating current with the driving frequency (f > 20 kHz) is applied to the spiral coil of the electromagnetic acoustic transducers. The dynamic magnetic field beneath the meander coil will be induced by the alternating current (within the electromagnetic skin depth). Generally, both the static magnetic field and the dynamic magnetic field will contribute to the Lorentz force occurring in skin depth. Generally, the skin depth is far less than the acoustic wavelength. Thus, the Lorentz force occurring within the skin depth can approximately be regarded as a shear stress exerted on the surface of the specimen, and the surficial stress can be regarded as an excitation source for the generation of a series of ultrasonic modes. In other words, the acoustic fields (the mechanical displacement) are generated by the Lorentz surface stress.

We consider nonlinear ultrasonic technique where the received signal is not at the frequency of the exciting current, and metallic material is treated as weakly nonlinear elastic because the amplitude of the signal received at higher harmonics is very small relative to the excitation, then harmonics can be generated notably at twice the excitation frequency.

The Lagrangian formulation from continuum mechanics is exploited using the Green-Lagrange strain tensor $\mathbf{E}$ along with the first Piola-Kirchhoff stress tensor $\mathbf{T}_1$ and second Piola-Kirchhoff stress tensor $\mathbf{T}_2$. $\mathbf{E}$ is related to the displacement vector $\mathbf{u}$, for simplicity, and the gradient of the displacement vector $\mathbf{H}$. And the following relations exist between the above quantities [25, 26].

$$\mathbf{E} = \frac{1}{2}\left(\mathbf{H} + \mathbf{H}^{\mathrm{T}} + \mathbf{H}^{\mathrm{T}}\mathbf{H}\right), \qquad \text{Equation 1}$$

where the linear strain is $\mathbf{E}^{\mathrm{l}}$, which is related to the action of linear ultrasonic.

$$\mathbf{E}^{\mathrm{l}} = \frac{1}{2}\left(\mathbf{H} + \mathbf{H}^{\mathrm{T}}\right). \qquad \text{Equation 2}$$

Comparing Equation 1 with Equation 2, the existence of the second-order term $\mathbf{H}^{\mathrm{T}}\mathbf{H}$ is the main reason of nonlinear stress-strain, which includes geometric nonlinearity and material nonlinearity.

The stress-strain relation of higher harmonic generation for a hyper-elastic material is obtained from the nonlinear governing equations of Murnaghan model, which has a qualitative description of an harmonic vibration, and the strain energy function $W(\mathbf{E})$ is

$$\begin{aligned} W(\mathbf{E}) = {} & \frac{1}{2}\lambda(\mathrm{tr}(\mathbf{E}))^2 + \mu\mathrm{tr}\left(\mathbf{E}^2\right) + \frac{1}{3}(l+2m)(\mathrm{tr}(\mathbf{E}))^3 \\ & - m\mathrm{tr}(\mathbf{E}) \times \left((\mathrm{tr}(\mathbf{E}))^2 - \mathrm{tr}\left(\mathbf{E}^2\right)\right) + n\det(\mathbf{E}), \end{aligned} \qquad \text{Equation 3}$$

where l, m, and n are Murnaghan constants, λ and μ are Lame's constants, and tr() and det() denote the trace and the determinant, respectively, of the bracketed tensor. The first Piola-Kirchhoff stress tensor and the second Piola-Kirchhoff stress tensor are obtained using

$$\mathbf{T}_1 = (\mathbf{I} + \mathbf{H})\mathbf{T}_2, \qquad \text{Equation 4}$$

$$\mathbf{T}_2 = \frac{\partial W(\mathbf{E})}{\partial \mathbf{E}}, \qquad \text{Equation 5}$$

where $\mathbf{I}$ is the second-order identity tensor. And $\mathbf{T}_1$ can be decomposed into linear and nonlinear components. Then the equation of motion in the reference configuration can be written as

$$\nabla \cdot \mathbf{T}_0 + \rho_0 \cdot \mathbf{b} = \rho_0 \ddot{\mathbf{u}}, \qquad \text{Equation 6}$$

$$\mathbf{b} = \mathbf{b}_{\mathrm{L,s}} + \mathbf{b}_{\mathrm{L,d}} = \mathbf{J}_{\mathrm{e}} \times \mathbf{B}_{\mathrm{s}} + \mathbf{J}_{\mathrm{e}} \times \mathbf{B}_{\mathrm{d}}, \qquad \text{Equation 7}$$

where ρ_0 is the mass density, $\ddot{\mathbf{u}} = \delta^2\mathbf{u}/\delta t^2$, and $\mathbf{b}$ is the Lorentz force which is the action of magnetic field (including the static magnetic field $\mathbf{B}_{\mathrm{s}}$ and the alternating magnetic field $\mathbf{B}_{\mathrm{d}}$) and eddy current. The calculated Lorentz force is then applied to the elasto-dynamic equation as a body load. The acoustic wave passes the material boundary and creates dynamic electromagnetic fields in a conductive material exposed to a steady magnetic field, which then can be detected by a received EMAT. The inverse effect applies whereby the acoustic wave forces the charged particles to move with the aid of the magnetic field of permanent magnet bias. The dynamic electric field induced by the acoustic field in a specimen and the equation of receiving voltage $\mathbf{E}$ can be written as

$$\mathbf{E} = \frac{\partial \mathbf{u}}{\partial t} \times \mathbf{B}_{\mathrm{s}}. \qquad \text{Equation 8}$$

3. NUMERICAL SIMULATIONS

In this section, the results are obtained from numerical simulations performed using COMSOL Multiphysics 4.3b, a commercial finite-element software. The schematic of the 2D model is shown in Figure 1. The modeling of Lorentz force generation process uses the *AC/DC*

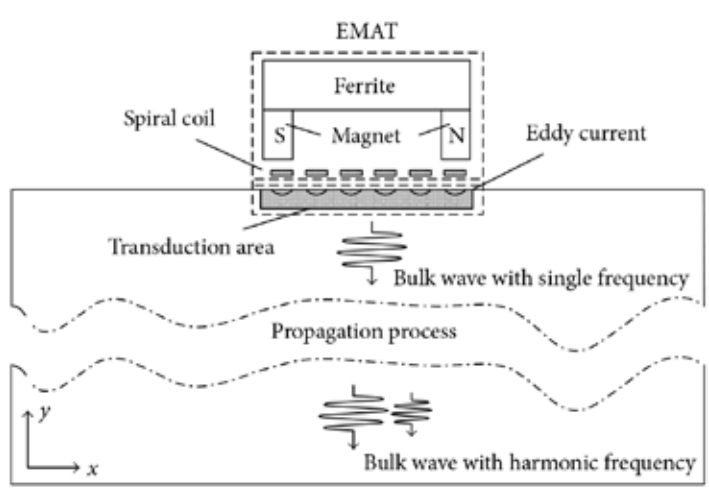

Figure 1: Schematic diagram of nonlinear EMAT finite element model.

Young's Modulus	Poisson's ratio	Electrical conductivity	ρ_0	λ	μ	l	m	n
70 GPa	0.33	37.7 MS/m	2700 kg/m^3	51 GPa	26 GPa	-250 GPa	-333 GPa	-350 GPa

Table 1: Elastic constants used for simulation.

Mechanisms	Constitutive	Description
Linear elastic material ("L" case)	$l = m = n = 0$ Linear strain E[1] (2)	No material or geometric nonlinearities are included
Nonlinear elastic material ("N" case)	$l \neq m \neq n \neq 0$ Green-Lagrange strain tensor E (1)	Both material or geometric nonlinearities are included
Geometrically nonlinear material ("G" case)	$l = m = n = 0$ Green-Lagrange strain tensor E (1)	Only geometric nonlinearities are included

Table 2: Three constitutive models.

and *Magnetic Fields* module, and the modeling of propagation process uses the *Structural Mechanics* module.

The electromagnetic acoustic transducer consists of a coil that provides a dynamic current and a U-shaped magnet providing a horizontal static magnetic field. While in the nonferromagnetic material, the ultrasonic wave is generated by the Lorentz forces. The Lorentz force is the interaction of the magnetic flux density and the eddy current. Thus, the electromagnetic field and mechanical field are coupled together by Lorentz forces in the transduction area.

The permanent magnet material feature is Nd-Fe-B with a remanence of 1.4 T. The horizontal static magnetic field acts parallel to the coil along the *x*-direction; there are also *x*-direction Lorentz forces present that are usually much smaller than that the *y*-direction Lorentz forces. The spiral coil consists of 35 wires with a diameter of 0.5mm and entangles together closely. The lift-off distance between the coil and the tested aluminum specimens is 0.5mm. The exciting coils are carrying a current signal of f = 500 kHz. The thickness of the transduction area is five times the skin depth, and a low reflecting boundary is used to reduce back reflections from the edge of the remote interfaces.

The ultrasonic wave is generated on the transduction area. The simulations were carried out using the Murnaghan model for aluminum, and the material properties are tabulated in Table 1. Quadrilateral elements are used to discretize the magnet and coil with a maximum element size of 0.5mm; the transduction area and propagation area are divided into triangular elements with a maximum element size of 0.1mm and 0.2mm.

3.1. Ultrasonic Wave Generation

Due to the match of the coil and magnet, Rayleigh waves (R-Waves) travel along the surface, and simultaneously, the longitudinal waves (L-Waves) and shear waves (S-Waves) travel vertically into the specimen. Since S-Waves do not transfer energy to second harmonics [27], we investigate the nonlinear action of L-Waves and the contribution of the L-Waves, which are based on the x-direction Lorentz forces.

The *x*-component of the displacement is denoted by displacement "*u*," the y-component is denoted by displacement "*v*," and the direction of L-Waves vibration keeps consistent with the direction of L-Waves travelling. So displacement "*v*" is only considered. Figure 2 shows the geometric dimension of the test specimen (100mm x 180mm) and the spread of ultrasonic wave inside the *x*- and *y*-coordinates which represent the cross-sectional displacement "*v*" view of the wave modes propagating in two transmission cycles (from t_0 to t_0+ 2T). The R-Waves velocity v_R, the S-Waves velocity v_S, and the L-Waves velocity v_L can be calculated by the time and the distance of flight between the two positions: v_R = 2,915 m/s, vS = 3,122 m/s, and v_L = 6,198 m/s. Thus, with the increase of propagation time, the separation of various ultrasonic waves is more clear.

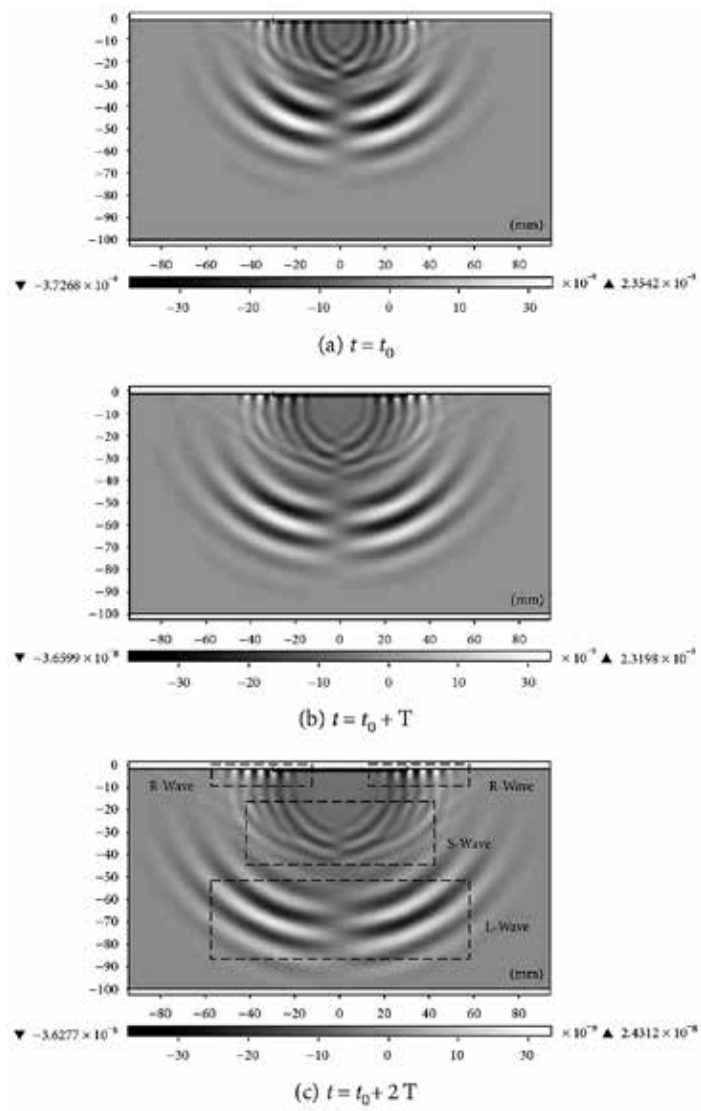

Figure 2: Ultrasonic wave displacement in aluminum plate generated by EMAT.

3.2. Nonlinear Ultrasonic Propagation

In typical EMAT configurations where the frequency is of the order from several hundreds of kHz to a few MHz, the amplitude of Lorentz force depends on the characteristic of the static magnetic field, the exciting current, the construction of the spiral coil, and the lift-off. In

order to eliminate the contribution of the second harmonic frequency due to alternating Lorentz force, the loading of body force is just applied by static Lorentz force $\mathbf{b}_{L,S}$ in numerical model. So, the results were obtained for ultrasonic wave at fundamental frequency. Then we discuss the contribution of material and geometric nonlinearities to the second harmonic generation in the specimen. The displacement "v" amplitude of L-waves should reach $1E-8$ m, and the exciting current condition chosen is 150 A; some nonlinear effects are not easily decipherable at lower amplitudes. The results for three nonlinear mechanisms are presented in Table 2.

Figure 3 illustrates the normalized time domain signal obtained for the displacement "v" at position (10 mm, -100 mm). It shows that the signals overlapped nearly for the three cases, and the difference is barely visible. So, the velocities of L-Waves are kept consistent in each. But in the frequency domain, as shown in the normalized logarithm processing of the fast Fourier transform (FFT) method in the figure, nonlinearity is evident from the nonlinear presence of zero-frequency and second harmonic components in the "v" displacement of "N" and "G" cases. And the amplitude of the second harmonic generated in the "N" case is several times greater than that generated in the "G" case. This shows that the second harmonic generation is dominated by the material nonlinearity as opposed to geometric nonlinearity. The same explanations were adapted to obtain the main mechanism of zero-frequency components, which is dominated by geometric nonlinearity, while the "L " case shows only fundamental frequency without any frequency components.

The displacement "v " were obtained at positions (10, -93.8 mm), (10, -100 mm), and (10, -106.2mm) where the length of each propagation distance is one fundamental L-Waves wavelength. Figure 4 shows the normalized time domain signal and normalized logarithm processing of FFT. As predicted by theory, the amplitude of the second harmonic increases with the propagation distance. Then we discussed the effect of scaling higher-order elastic constants on the harmonic generation that increases with the degree of material damage.

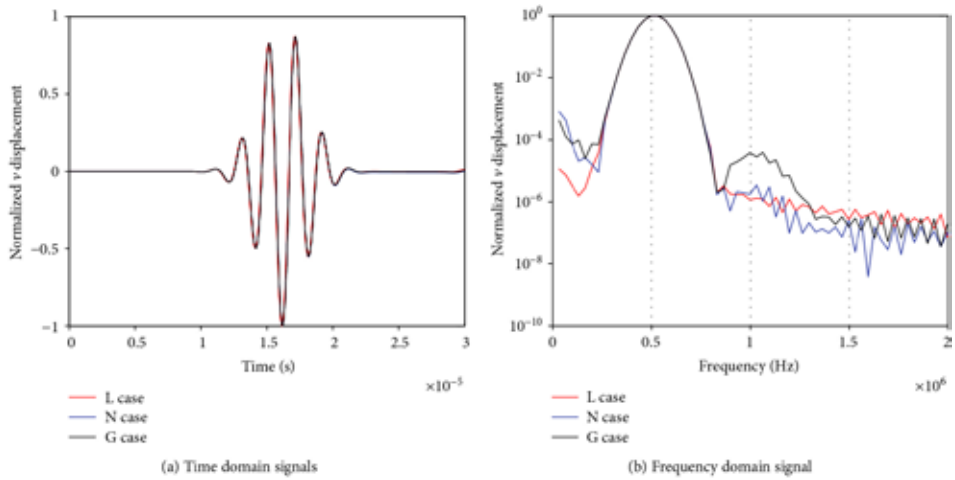

Figure 3: L-Waves signals obtained using LE, NL, and NG constitutive model.

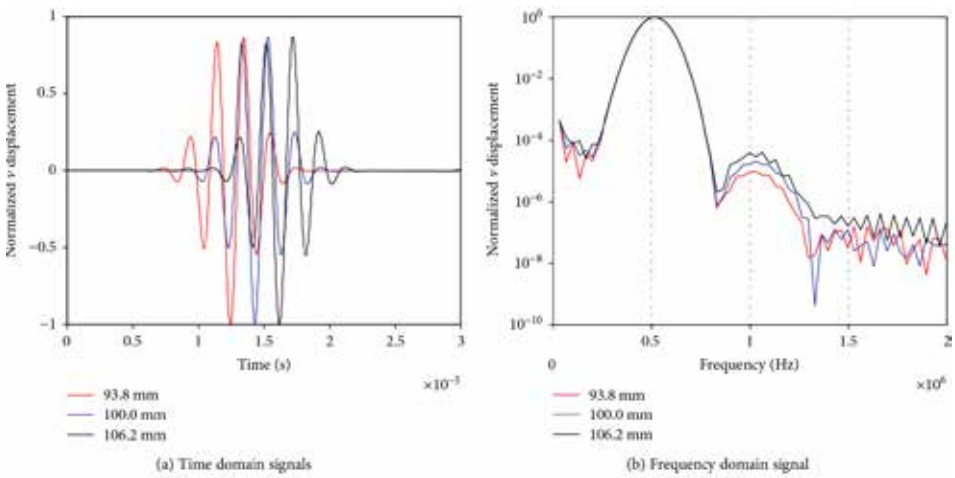

Figure 4: L-Waves signals at 93.8, 100.0, and 106.2 mm from the surface of the plate.

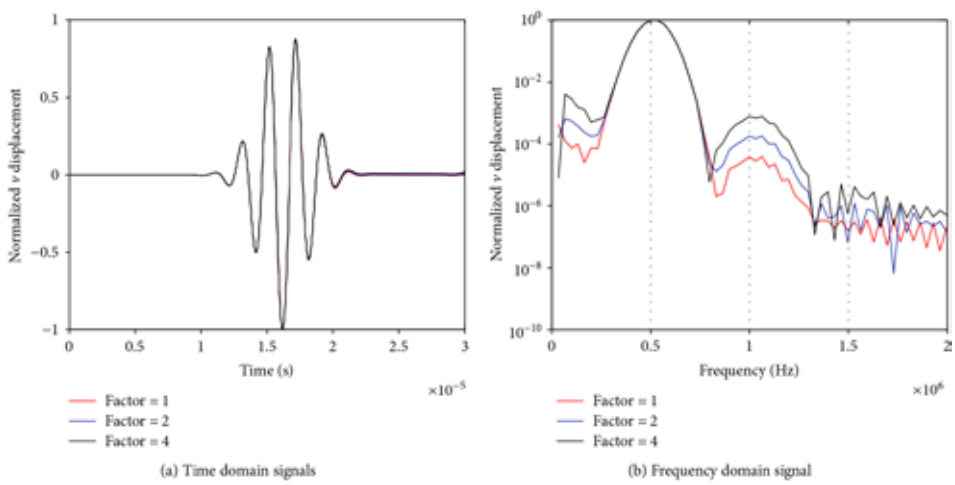

Figure 5: L-Waves signals obtained by scaling Murnaghan constants by factors of 1, 2, and 4.

Simulations for the "N " case used three different sets of higher-order elastic constants obtained by scaling Murnaghan constants by factors of 1, 2, and 4. Figure 5 shows the normalized time domain signal and normalized logarithm processing of FFT. As shown, the zero-frequency and second harmonic components are increasing with the factors. From another perspective, the degree of material damage increases with the nonlinear effects. In the following example, we present the results obtained for the second harmonic generation from the L-Waves at 500 kHz, 600 kHz, and 800 kHz in the "N " case. As shown in Figure 6, the same presence of zero frequency and second harmonic components in the various frequencies, and the normalized amplitudes of zero frequency and second harmonic components remain the same.

4. EXPERIMENTAL SECTION

4.1. Sample Preparation

Tensile specimens made of aluminum alloy 6061 were fabricated

Specimen number	Loading F_{max} (KN)	Strain rate v (mm/min)	Loading time t (s)
A_0	0	0	0
A_1	24.488	5	25.422
A_2	47.710	5	52.328
A_3	54.008	5	76.000
A_4	53.232	5	95.031

Table 3: Condition of strain induced in specimens.

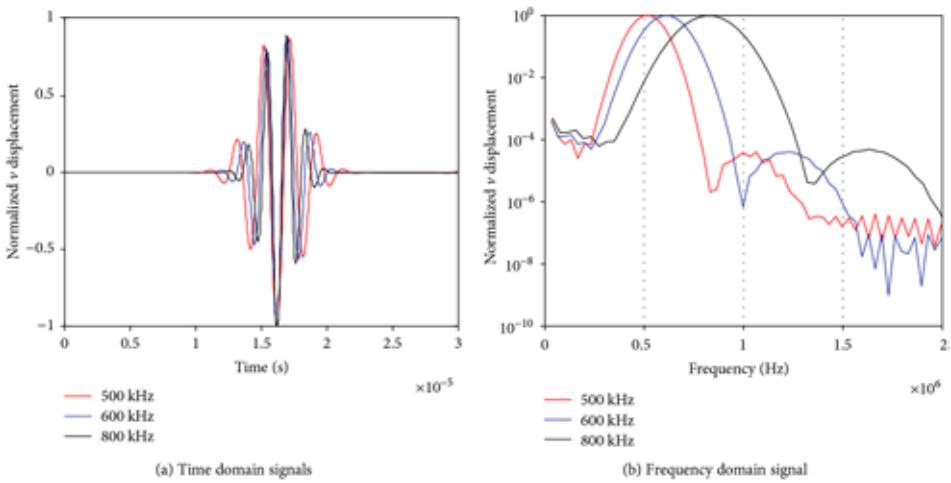

Figure 6: L-Waves signals obtained at f = 500 kHz, 600 kHz, and 800 kHz.

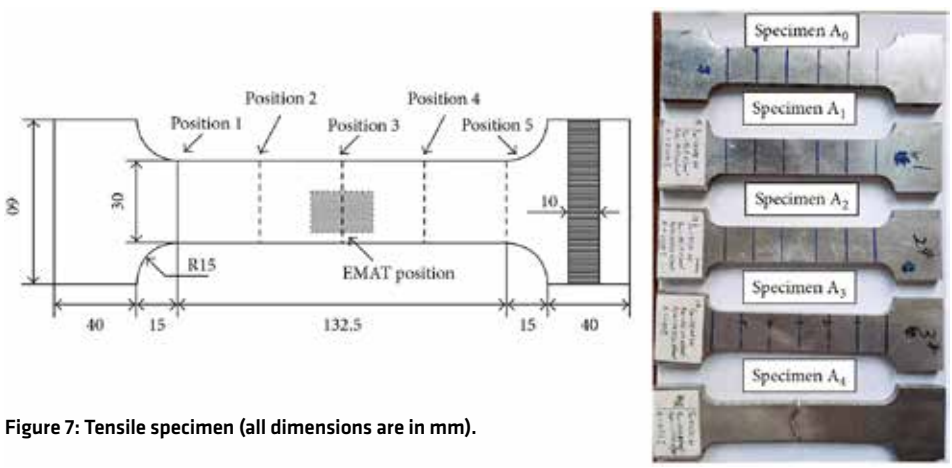

Figure 7: Tensile specimen (all dimensions are in mm).

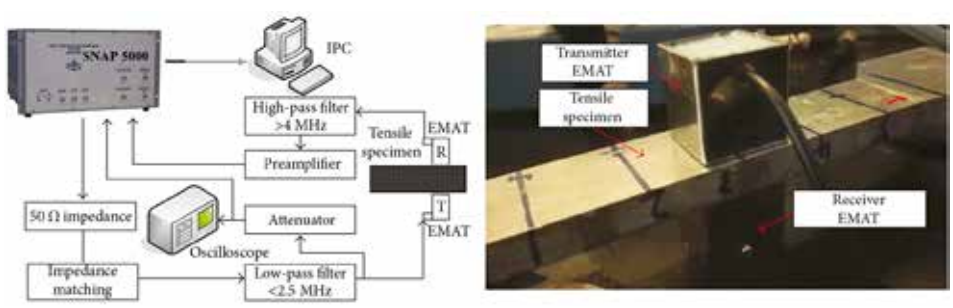

Figure 8: Block diagram of the experimental system construction.

for conducting the plastic deformation studies. The specimens were tensile loaded to various levels of elastic-plastic strain under strain control, as shown in Table 3. Among them, A_0 was an undamaged specimen; A_1 was a specimen which produced in the elastic tensile area; A_2 was a specimen that produced in the elastic-plastic critical tensile area; A_3 was a specimen that produced in the plastic tensile area, and A_4 was a fractured specimen. The noncontact nonlinear characteristics were evaluated after unloading these specimens.

Nonlinear longitudinal wave was monitored at different positions along the length direction of tensile specimens for each sample. Figure 7 shows the positions of measurement along the thickness direction; each position is evenly spaced. The specimens are subjected to a uniaxial tensile test. The deformation is such that the material presents an elastoplastic behavior with nonlinear isotropic hardening. When subjected to such large deformations, the specimen experiences a significant plastic deformation and necking in its central cross section, and so nonlinear ultrasonic wave response at each position is various for one loading condition.

4.2. Nonlinear Ultrasonic Measurement Strategy

Figure 8 shows the nonlinear electromagnetic acoustic measurement. The nonlinear response of tensile specimen aluminum alloy was excited by using a RITEC SNAP RAM-5000 high power system (RITEC Inc., Warwick, RI, USA), and the high amplitude sinusoidal tone burst inputs with a few number of cycles at a stable single frequency.

A pair of EMAT transducers are placed on the double sides of the specimen (through the thickness) as shown in Figure 9.

The EMAT transducer is mainly combined by a coil and permanent magnet. A toothpick is used to wind the copper wire with a diameter of 0.1mm; each turn is paralleled so closely that a large radius of spiral coil is obtained. The spiral shape of the EMAT coil is kept by laying an epoxy adhesion bond. BNC cable is connected to the spiral coil, and the permanent magnet is put on top of the coil. The bulk EMAT is facilitated after padding insulating polymer. The combination of a U-shape magnet provides a horizontal-bias magnetic field, and the spiral coil exerts high-frequency current excitation, so the electromagnetic force is mainly in a vertical direction; the particle in the skin depth will be affected by the electromagnetic force and produce a high vertical frequency vibration. The high vertical vibration producing ultrasonic bulk waves would spread in the specimen. One of the transducers acts as the transmitter, sending the bulk wave (mainly, longitudinal wave) across the specimen, and the other transducer plays the role as the receiver based on the principle of electromagnetic induction. Hence, the longitudinal wave propagates along the thickness direction of the specimen, and the received longitudinal wave would contain nonlinear information through the propagation path.

However, since this measurement by noncontact method EMAT has lower transduction efficiency, to avoid this inconvenience, additional devices are required to maintain the noncontact method by impedance matching and a high-pass filter. The exciting current has

no window function in order to improve the exciting energy, which are from the high-power system to the EMAT transducers. Meanwhile, the exciting frequency should be considered by the designed EMAT frequency spectrum response curve as shown in Figure 10. These two EMAT transducers have the same designed size; thus, the exciting frequency has to be set 2.2 MHz, and the fundamental frequency 2.2MHz and the harmonic frequency 4.4MHz can be received at the peak frequency spectrum.

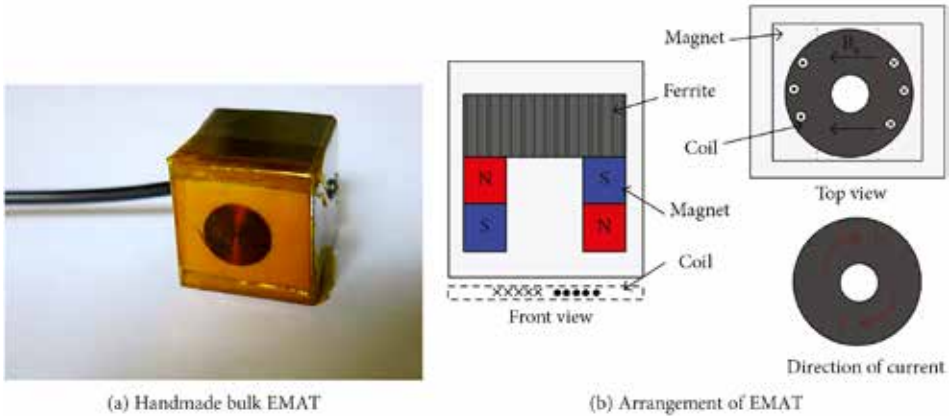

Figure 9: Physical diagram of spiral electromagnetic acoustic transducer.

5. ANALYSIS

Nonlinear longitudinal wave measurement along the thickness direction of the Al 6061 plates are performed with the EMAT and PZT setup, and no near sound field effects are observed in this experimental setup with the suited selection of exciting condition.

5.1. Nonlinear PZT Measurement

The nonlinear parameter β indicates that a linear relationship between the second harmonic amplitude A_2 and the square of the fundamental amplitude (A_1^2). Since measurement of fundamental and second harmonic response by received ultrasonic sensor is in terms of the several voltages excitation, and β can be predicted by the microplasticity model as a function of the tensile stress with few influence of different exciting frequencies [7], so a 5MHz excited PZT sensor and a 10MHz received PZT sensor were employed through the thickness direction to implement generated longitudinal wave.

Figure 11 shows a variation amplitude of A_2 with A_1^2 at the position 3 of specimen A_0; the black spots are experimental data points at 10~50 level exciting voltages, and a linear fitting line of A_2 vs. A_1^2 for different driving voltages is clearly obtained, which means that the nonlinear parameter keeps constant for different voltages. The slope of this linear fitting line is the value of the nonlinear parameter β_{p0}, and β_{p0} mainly includes material nonlinearity β_{p0} and contact nonlinearity β_{c0} .

Consider the fluctuation of frequency response curve of PZT sensors (the frequency response at 5MHz and 10MHz points have disaffinity) and the influence of the nonuniform unit. Hence, the normalized nonlinear coefficient is β'_{p0} (the ratio between the nonlinear parameter measured in the tensile damage specimen to β_{p0}), that is, $\beta'_{p0} = \beta_p/\beta_{p0}$.

5.2. Compared with Nonlinear EMAT Measurement

In this EMAT measurement study, the lower transduction efficiency of EMAT is considered, as shown in Figure 12. EMAT has low energy converting efficiency and is sensitive to noise.

The noise interference is mainly composed of continuous interference noise, paroxysmal interference noise, and electromagnetic noise, which are generated by the operation of the tested equipment and alternating electromagnetic fields in the limited space volume of the electromagnetic ultrasonic transducer. In order to realize the effective recognition of ultrasonic echo signal, the frequency-domain signal needs to be received with 40 dB attenuation of low-frequency stage and 60 dB amplification of high-frequency stage, where one can clearly find the contributions of the fundamental and second harmonic waves. Meanwhile, the frequency domain signal is filled with noise spectrum. To obtain the amplitudes of the fundamental and second harmonic wave components, Daubechies wavelet function and third wavelet packet decomposition levels were adopted to denoise as shown in Figure 12. In order to compare with the measurement by PZT sensor, and the nonlinear parameter β_{E0} should be

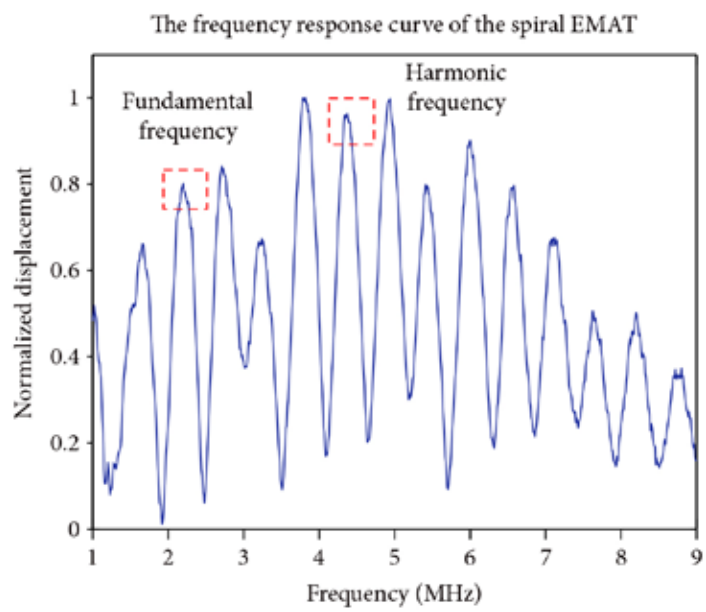

Figure 10: Frequency response curve of spiral electromagnetic acoustic transducer.

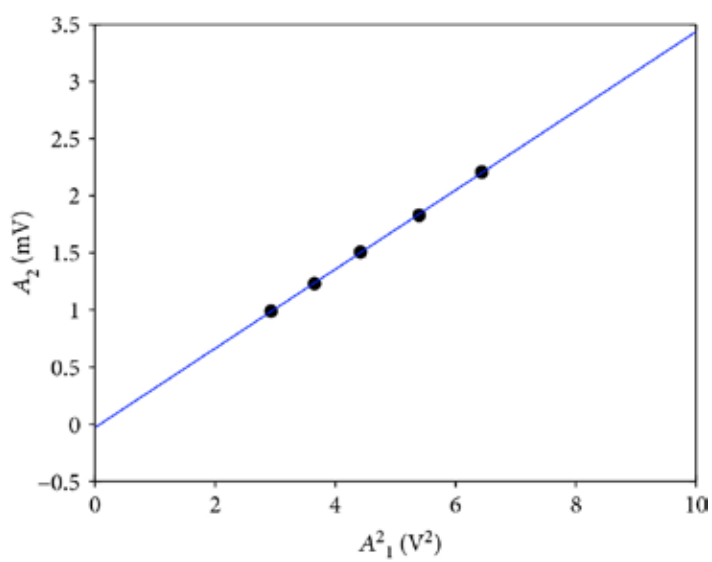

Figure 11: The linear variation of A_2 with A_1^2.

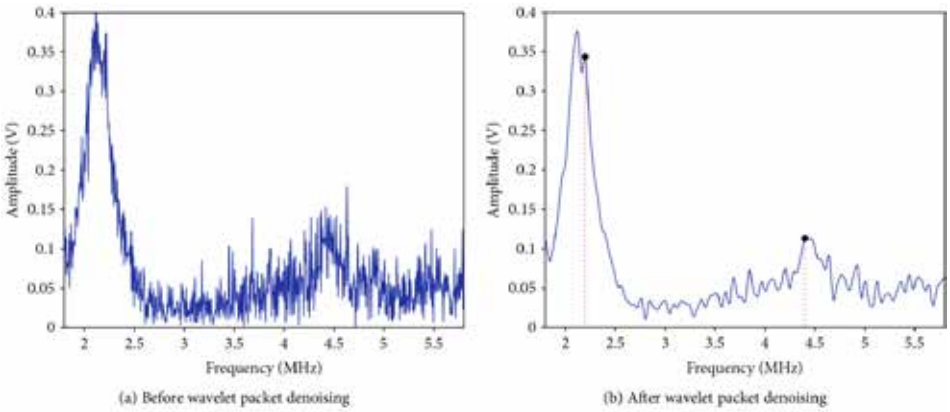

Figure 12: Frequency spectrum characteristic in nonlinear EMAT experiment.

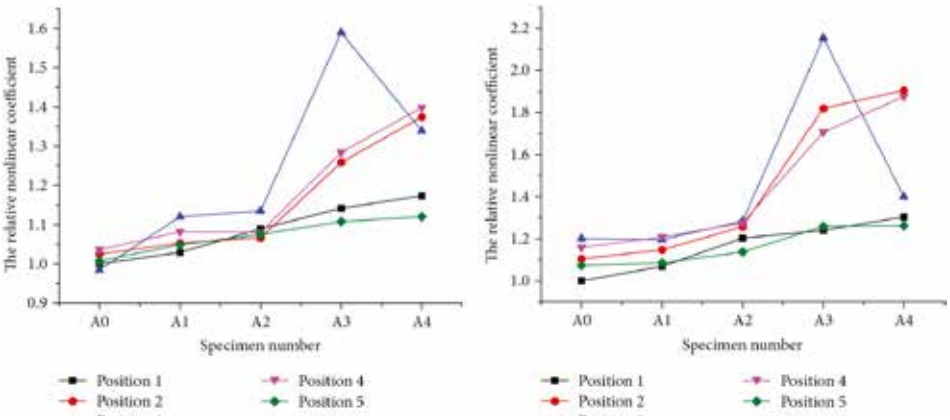

Figure 13: The relative nonlinear coefficient.

From the experimental perspective, this research demonstrates the feasibility and robustness of noncontact EMAT method for the nonlinearity measurement with a longitudinal wave.

normalization processing by noncontact EMAT measurement, the normalized nonlinear coefficient $\beta'_{E0}=\beta_E/\beta_{E0}$.

Figure 13 shows the comparison of the relative nonlinear coefficients by the two methods. With the same loading, the variation tendency of the relative nonlinear coefficients stayed the same.

With elastic tensile loading (F_{max} < 47.71 kN), the relative nonlinear coefficients nearly keeps unchanged; thus, the elastic constant changes very little and increases rapidly when the tensile loading exceeds 47.71 kN at the position of 2, 3, and 4. Plastic deformation starts to exist at these positions; meanwhile, the relative nonlinear coefficients change very little at positions 1 and 5. It can be found that the plastic deformation is symmetrically distributed along the center specimen position (position 3) by tensile loading, and based on the metal necking effect, the plastic deformation is most notable at position 3. When the tensile loading exceeds 53.232 kN, the relative nonlinear coefficient drops rapidly, occurring with the more discontinuous area; at the same time, the plastic deformations at the position of 2 and 4 are still in the hardening stage and the relative nonlinear coefficients are still increasing.

It can be seen that the EMAT ultrasonic measurement is bigger than that of the PZT ultrasonic measurement. Namely, $\beta'_{E0} > \beta'_{p0}$, compared with what constitutes the two relative nonlinear coefficients, it is the contact nonlinearity (the influence of couplant and rough surface), which mainly causes the decrease in relative nonlinear coefficients. The result also shows that the change of the plastic nonlinearity on the plastic deformation can be measured using the proposed noncontact ultrasonic method, and the relative nonlinear coefficients measured by EMAT ultrasonic have potential applications in detecting variation tendency of plastic deformation under extreme environments.

6. CONCLUSIONS

In this article, tensile damage behavior of nonlinear longitudinal wave was investigated. From the numerical perspective, simulations of EMAT transduction and ultrasonic wave propagation were carried out in COMSOL Multiphysics 4.3b using the Murnaghan hyperelasticity model, harmonic generation from the fundamental longitudinal wave, while time domain signals show very small difference. The contribution of material nonlinearity, geometric nonlinearity, damage cased nonlinearity, and propagation distance cased nonlinearity to the harmonic generation is discussed. As the accumulated material damage is typically inferred from the nonlinear coefficient, which in turn depends on the higher Murnaghan constants and longer propagation distances, the exciting frequency is not inferred from the nonlinear coefficient.

From the experimental perspective, this research demonstrates the feasibility and robustness of noncontact EMAT method for the nonlinearity measurement with a longitudinal wave; thus, the surface condition of the specimen is relatively not important. The experimental setup provides an output signal with low SNR; meanwhile, wavelet denoising method can improve the SNR and extract nonlinearity information from measuring frequency signals.

The results obtained in this research demonstrate that the noncontact, EMAT detection method provides potential field applicability for the in-situ measurements of the relative nonlinearity parameter in online structures. Further work needs to be done to identify the fatigue damage of ferromagnetic structure by EMAT method based on the magneto-strictive mechanism.

CONFLICTS OF INTEREST

The authors declare that there is no conflict of interest regarding the publication of this paper.

ACKNOWLEDGMENTS

This work was supported by the Natural Science Foundation of Jiangxi Province (Grant no. 20171BAB216035) and Science Foundation of Jiangxi Provincial Department of Education "Plastic damage detection method in metallic components based on electromagnetic transduction". (Grant no. GJJ170409).

REFERENCES

[1] L. R. Joseph, Ultrasonic Guided Waves in Solid Media, Cambridge University Press, New York, NY, USA, 2014.

[2] K. H. Matlack, J. Y. Kim, L. J. Jacobs, and J. Qu, "Review of second harmonic generation measurement techniques for material state determination in metals," Journal of Nondestructive Evaluation, vol. 34, no. 1, p. 273, 2015.

[3] J. H. Cantrell and W. T. Yost, "Effect of precipitate coherency strains on acoustic harmonic generation," Journal of Applied Physics, vol. 81, no. 7, pp. 2957–2962, 1997.

[4] J. S. Valluri, K. Balasubramaniam, and R. V. Prakash, "Creep damage characterization using non-linear ultrasonic techniques," ActaMaterialia., vol. 58, no. 6, pp. 2079–2090, 2010.

[5] G. Shui, Y. Wang, P. Huang, and J. Qu, "Nonlinear ultrasonic evaluation of the fatigue damage of adhesive joints," NDT & E International, vol. 70, pp. 9–15, 2015.

[6] X. Wan, Q. Zhang, G. Xu, and P. W. Tse, "Numerical simulation of nonlinear lamb waves used in a thin plate for detecting buried micro-cracks," Sensors, vol. 14, no. 12, pp. 8528–8546, 2014.

[7] A. Ruiz, N. Ortiz, A. Medina, J. Y. Kim, and L. J. Jacobs, "Application of ultrasonic methods for early detection of thermal damage in 2205 duplex stainless steel," NDT and E International., vol. 54, pp. 19–26, 2013.

[8] G. Shui, Y. Wang, and F. Gong, "Evaluation of plastic damage for metallic materials under tensile load using nonlinear longitudinal waves," NDT & E International., vol. 55, pp. 1–8, 2013.

[9] J. Frouin, S. Sathish, T. E. Matikas, and J. K. Na, "Ultrasonic linear and nonlinear behavior of fatigued Ti–6Al–4V," Journal of Materials Research., vol. 14, no. 4, pp. 1295–1298, 1999.

[10] H. Jeong, S. H. Nahm, K. Y. Jhang, and Y. H. Nam, "A nondestructive method for estimation of the fracture toughness of CrMoV rotor steels based on ultrasonic nonlinearity," Ultrasonics, vol. 41, no. 7, pp. 543–549, 2003.

[11] D. C. Hurley, D. Balzar, and P. T. Purtscher, "Nonlinear ultrasonic assessment of precipitation hardening in ASTM A710 steel," Journal of Materials Research., vol. 15, no. 9, pp. 2036–2042, 2000.

[12] J. Y. Kim, L. J. Jacobs, J. M. Qu, and J. W. Littles, "Experimental characterization of fatigue damage in a nickel-base superalloy using nonlinear ultrasonic waves," The Journal of the Acoustical Society of America., vol. 120, no. 3, pp. 1266–1273, 2006.

[13] C. Pruell, J. Y. Kim, J. Qu, and L. J. Jacobs, "A nonlinear-guided wave technique for evaluating plasticity-driven material damage in a metal plate," NDT and E International., vol. 42, no. 3, pp. 199–203, 2009.

[14] G. Choi, Y. Liu, X. Yao, and C. J. Lissenden, "Effect of localized microstructural evolution on higher harmonic generation of guided wave modes," in 41st annual review of progress in quantitative nondestructive evaluation, pp. 1592–1598, Boise Idah, USA, 2014.

[15] T. Sebastian, J. Y. Kim, J. M. Qu, and L. J. Jacobs, "Air-coupled detection of nonlinear Rayleigh surface waves to assess material nonlinearity," Ultrasonics, vol. 54, no. 6, pp. 1470–1475, 2014.

[16] P. Liu, H. Sohn, T. Kundu, and S. Yang, "Noncontact detection of fatigue cracks by laser nonlinear wave modulation spectroscopy (LNWMS)," NDT & E International, vol. 66, pp. 106– 116, 2014.

[17] M. Hirao and H. Ogi, Electromagnetic Acoustic Transducers: Noncontacting Ultrasonic Measurement Using EMATs, Springer, KK, Japan, Second Edition edition, 2016.

[18] M. Kogia, T. H. Gan, L. M. Balachandran et al., "High temperature shear horizontal electromagnetic acoustic transducer for guided wave inspection," Sensors, vol. 16, no. 12, p. 582, 2016.

[19] H. Ogi, T. Ohtani, and S. Aoki, "Noncontact monitoring of surface-wave nonlinearity for predicting the remaining life of fatigued steels," Journal of Applied Physics, vol. 90, no. 1, pp. 438–442, 2001.

[20] T. Ohtani, H. Ogi, and M. Hirao, "Noncontact evaluation of surface-wave nonlinearity for creep damage in Cr-Mo-V steel," Japanese Journal of Applied Physics, vol. 48, no. 7, article 07GD02, 2009.

[21] A. Cobb, M. Capps, C. Duffer, J. Feiger, K. Robinson, and B. Hollingshaus, "Nonlinear ultrasonic measurements with EMATs for detecting pre-cracking fatigue damage," in Review of Progress in Quantitative Nondestructive Evaluation, vol. 1430, pp. 299–306, Burlington, VT, USA, 2012.

[22] A. Cobb, E. Macha, J. Bartlett, and Y. Xia, "Detecting sensitization in aluminum alloys using acoustic resonance and EMAT ultrasound," in , Article ID 05000143rd annual review of progress in quantitative nondestructive Evaluation, vol. 1806, Atlanta, GA, USA, 2016.

[23] C. Pei, P. Xiao, S. Zhao, and Z. Chen, "Development of a flexible film electromagnetic acoustic transducer for nondestructive testing," Sensors and Actuators A: Physical., vol. 258, pp. 68–73, 2017.

[24] D. Rueter, "Experimental demonstration and circuitry for a very compact coil-only pulse Echo EMAT," Sensors, vol. 17, no. 12, p. 926, 2017.

[25] V. K. Chillara and C. J. Lissenden, "Nonlinear guided waves in plates: a numerical perspective," Ultrasonics, vol. 54, no. 6, pp. 1553–1558, 2014.

[26] K. Zhang, P. X. Yi, Y. H. Li, B. Hui, and X. Zhang, "A new method to evaluate surface defects with an electromagnetic acoustic transducer," Sensors, vol. 15, no. 12, pp. 17420– 17432, 2015.

[27] L. Yang, V. K. Chillara, C. J. Lissenden, and L. Joseph, "Third harmonic shear horizontal and Rayleigh lamb waves in weakly nonlinear plates," Journal of Applied Physics, vol. 114, no. 11, article 114908, 2013.

ABOUT THE AUTHORS

Zhichao Cai and Hao Cheng are with the School of Electrical and Automation Engineering, East China Jiaotong University, Nanchang 330013, China. Chengcheng Liu is with the State Key Laboratory of Reliability and Intelligence of Electrical Equipment, Hebei University of Technology, Tianjin 300130, China. Correspondence should be addressed to Zhichao Cai; czchebut@foxmail.com.

Received July 19, 2017; accepted December 26, 2017; published April 10, 2018; academic editor: Emad Elbeltagi.

The article was edited to conform to the style of Thermal Processing magazine. The original article is available at: www.hindawi.com/journals/js/2018/1745257.

COMPANY PROFILE ///

CERAMATERIALS

DELIVERING ELITE SERVICE AND COST PERFORMANCE

Multi-Tiered CFC Fixture with removable posts engineered by CeraMaterials. (Courtesy: CeraMaterials)

CeraMaterials is a global manufacturing, distribution, and engineering outfit specializing in high-temperature refractory materials including: CFC, graphite insulation, machined graphite, ceramic fiber, TZM, sintered ceramics, mineral wool, fire brick, and other common refractory materials, coatings, and accessories.

By KENNETH CARTER, Thermal Processing editor

CeraMaterials opened its doors 12 years ago, and during that time, has become a major player for the heat-treat industry. A key ingredient to that success can be reduced down to a simple concept: listening.

"What we try to do that I think a lot of companies miss, and it's very basic, is actively listen," said Jeff Opitz, president of CeraMaterials. "When a customer comes to us with a problem or a material request, we're very intentional about understanding what our customer is asking for, and then rapidly responding with an appropriate solution."

And that quick response time is crucial to CeraMaterials' effectiveness and success as well.

"In many cases we're dealing with a maintenance manager or production engineer who has equipment down" Opitz said. "In the heat-treating business, down time is toxic, so we work fast. Our shipping department is geared up to ship all the way until 4 p.m. same day, so if a customer calls us at 3:30 p.m. needing a few CFC threaded bolts for their vacuum furnace overnighted, we get it done."

EXTENSIVE PRODUCT RANGE

CeraMaterials offers a full range of products for vacuum and protective atmosphere environments.

"Speaking broadly, we offer any aftermarket component utilized in a moly or graphite hot zone — this ranges from insulation packages, to heating elements, to hearth rails and everything in between" he said. "We are also heavily involved with fixturing — the shelves or grids that hold the work. Because of its light weight, low thermal mass, and excellent resistance to distortion, CFC is an ideal material for fixturing — we've been busy assisting customers with conversions this year."

CeraMaterials also has a wide range of products for atmosphere heat treaters and steel manufacturers, according to Opitz.

"We stock a myriad of refractory brick chemistries — ceramic blanket, ceramic paper, ceramic modules, ceramic fiber textiles, mortars, and castable mixes" he said. "Basically, any material or part inside a furnace, we're supplying."

ONE-STOP SHOP

And in addition to its wide range of product offerings, CeraMaterials aims to be even more to its customers, according to Opitz.

"We want to be a company that a maintenance manager can call, a mechanical engineer can call, a procurement officer can call and source all the materials that they need for their operation from one place," he said. "That's why our tag line is 'Your One-Stop Shop for Thermal Processing.' We have a deep product line, and if something's not listed on our website, chances are we can help provide it. Our customers love the fact they can come to us and buy everything they need rather than dealing with five or six separate companies. They either give us a phone call or come to our website, and everything they need is right there."

CeraMaterials President Jeff Opitz holds a 2.5D Carbon/Carbon Grid. (Courtesy: CeraMaterials)

Opitz stressed that CeraMaterials is extremely customer-centric.

"Our primary mission is providing service to our customers," he said. "We make sure that when a call comes in, you're not getting an automated system or voice prompt menu; a competent human answers the phone, and we strive for it to be on the very first ring. It's kind of old school, but that's important to us. When someone calls, we want them to interact directly with a member of our team who can get them answers immediately."

That customer-centric philosophy doesn't end with phone calls. It applies to all the ways a customer might reach out for assistance, according to Opitz.

"When RFQs come in via email, we acknowledge the receipt of

"Because of our broad reach, we tend to have a good feel for what's happening in the industry."

The recent construction of CeraMaterials' new distribution facility in northeastern Pennsylvania gives the company 20,000 square feet of warehouse sapce and 5,000 square feet of office space. (Courtesy: CeraMaterials)

quote within five minutes and usually get the quote turned around in no more than 24 hours," he said. "It's about speed, service, and providing customers with an overall positive experience."

BUILDING ON EXPERIENCE

And yet another aspect of working closely with its customers is how CeraMaterials uses that knowledge to collectively collaborate, according to Opitz.

"Because of our broad reach, we tend to have a good feel for what's happening in the industry," he said. "We try to learn from our heat-treating community what the current trends are. Maybe in a pinch, instead of replacing an entire insulation board, we can get away with using some of our graphite moldable mix to get you up and running again. It's just understanding what's happening and getting customers out of jams. That's what we're all about."

For the last several years, CeraMaterials has been developing its own line of graphite coatings and adhesives and treatments, according to Opitz.

"We used to source these products from different companies but were never thrilled with any of them, so we started making our own," he said. "Seeing that product line developed — our EBS series of adhesives and coatings — has been rewarding. We're steadily establishing ourselves in the market."

FROM SOURCING TO SELLING

CeraMaterials was founded by Dr. Jerry Weinstein, who was originally hired to consult with a company making body armor. The company, Ceradyne, was having difficulty sourcing some of the raw materials it needed, so it hired Weinstein to source the material.

Once Weinstein had found it, he convinced Ceradyne to allow him to sell the material outright instead of dealing with consulting fees. And Ceradyne agreed, according to Opitz.

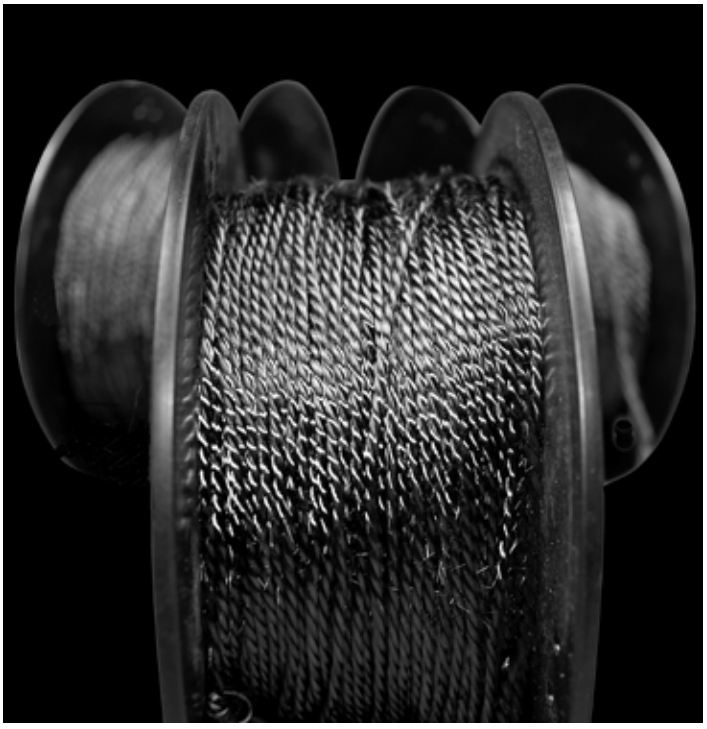

CeraMaterials new 24k tight weave carbon cordage offers superior tensile strength. (Courtesy: CeraMaterials)

"That was our first customer, our first order," he said. "That's how we kind of got up and running in the high-temp material game. And then from there, the growth was organic. We identified needs in the

Ceramic Fiber Blanket is available in varying grades, densities, and temperature ratings. (Courtesy: CeraMaterials)

marketplace and started offering what customers were asking for."

QUICK RISE TO SUCCESS

In 12 years, however, Opitz points out that CeraMaterials has become a major player.

"We have a diverse roster of high-profile "household-name" customers, government branches, national labs and universities, and have affiliations with most of the big names in the North American heat-treating world; it's been a decade of growth," he said.

A visible symbol of that growth can be seen in CeraMaterials' recent construction of a new distribution facility in northeastern Pennsylvania, according to Opitz.

"We went from a relatively small space to now having 20,000 square feet of warehouse and 5,000 square feet of office space; it was a massive construction project," he said. "It took us about two years from start to finish, but the facility is something I'm extremely proud of. It enables us to carry more inventory and fabricate more efficiently, both of which benefit our customers. We have an excellent group of people here, from materials engineers to customer service reps to the shipping department. They're happy working here because it's a nice environment."

CeraMaterials is certainly not content with even that recent expansion, and Opitz said he expects the company to grow as the industry does. Part of that growth will more than likely involve the virtual side of heat treat. The company is also looking into setting up a warehouse in Mexico or near the border that will allow CeraMaterials to serve that market as well.

And from a digital standpoint, CeraMaterials recently launched a completely revamped e-commerce website and is in the process of creating four additional websites that will focus on more specific niche categories, according to Opitz.

"It improves our SEO metrics," he said. "With more hooks in the water, you're going to catch more fish."

MORE INFO ceramaterials.com

MARKETPLACE ///

Manufacturing excellence through quality, integration, materials, maintenance, education, and speed.

Contact **Thermal Processing** at 800-366-2185 to feature your business in the Marketplace.

ADVERTISER INDEX ///

RAYMOND DANIEL NOBLE /// VICE PRESIDENT /// NOBLE INDUSTRIAL FURNACE

"Much of what we build is built to design, and nothing makes us prouder than when we deliver a quality product that meets or exceeds our customers' expectations."

What are your duties with Noble Industrial Furnace? What is your typical day?

My duties include, but are not limited to, oversight of design and construction of our new builds along with leading contracting crews on the road. We are a leading manufacturing company that continues to have roots in the field servicing all types of heat treat furnaces and equipment.

My typical day begins with coffee and emails then helping the crews get loaded up and out the door. With a steady flow of simultaneous projects in the shop, there is always something to do from ordering parts, double checking prints to helping weld pipe or lay brick. When not in the shop, you'll find me in the front office working with our design team, writing equipment proposals, and taking time to connect with our customers and vendors.

What products and services does Noble Industrial Furnace offer?

Noble provides industries worldwide with a full range of customized industrial thermal processing equipment. We build, repair, and maintain all typical batch furnace designs along with belt and tube furnaces.

After consulting with each customer, Noble provides customized furnace designs that incorporate the needs of the customer. Once the furnace concept and drawings have been accepted, work begins, and Noble takes over the project until its completion. All aspects of the construction, installation, testing, and training of the furnace are handled by Noble Industrial Furnace. Only when our customer's end users are up and running does Noble consider the job complete.

Noble also specializes in furnace refurbishment. When acquiring a new furnace or system is not budget friendly, customers choose Noble to refurbish a furnace. Refurbishing a furnace transforms a worn and outdated piece of equipment into a high-performance furnace meeting all updated safety and control regulations.

We also offer on-site emergency and scheduled repairs of all types of thermal processing equipment with minimal downtime to get our clients back up and running as soon as possible.

Noble has also responded to our customers' needs by providing preventative maintenance programs. These annual or semi-annual services include completion of all necessary maintenance, a thorough inspection of the equipment, and a detailed inspection report of our findings and maintenance performed.

What is Noble doing to advance the heat-treat industry?

We have been perfecting our design for gas and electric coating furnaces for the aerospace and ground-based turbine industries. Our close partnership with Lachance Controls for the past 35 years has helped bring us into the position where we can produce state-of-the-art equipment. Such systems have been sought out and purchased by the top turbine and engine builders in the world.

What are some of Noble Industrial Furnace's proudest moments?

Much of what we build is built to design, and nothing makes us prouder than when we deliver a quality product that meets or exceeds our customers' expectations. Most times, after a furnace is put in production, we visit our customer's facilities and have the opportunity to engage with the people who use our equipment each day. It's the feedback we get from those visits that makes us truly proud and committed to what we do.

We have built some great furnaces and these furnaces have lasted. And in many cases these furnaces have continued in production with changes in supervision, process, and location. Knowing we have designed, fabricated, and installed furnace systems both domestically and internationally along with meeting the many challenges of furnace design, including performance, size, uniformity, and process, makes us proud of our accomplishments.

What sets Noble Industrial Furnace apart when it comes to what you can offer a customer?

We know our furnaces. Every cut and weld, each component from brick to bolt, every burner and element, each valve, switch, and regulator is set in place by a skilled member of our team.

We know our customers. Having close relationships with our customers is an integral part of ensuring the equipment delivers. We have worked with many of our customers for multiple decades.

We know the industry. With over 175 years of combined experience in designing, building, and installing industrial thermal-processing equipment, there are very few things we have not seen. We provide our customers with products specifically designed to perform at or beyond their requirements.

MORE INFO noblefurnace.com